A Route to a Cyclobutane-Linked Double-Looped System via a Helical Macrocycle
Jan Klajn, Wojciech Stawski, Piotr J. Chmielewski, Joanna Cybińska and Miłosz Pawlicki

Contents

1. General Information

NMR Spectroscopy. 1 H NMR spectra were recorded on a high-field spectrometers (^{1}H 600.15 MHz and 500 MHz, ^{13}C 150 MHz), equipped with a broadband inverse gradient probehead. Spectra were referenced to the residual solvent signal (chloroform-d, 7.24 ppm). Two dimensional NMR spectra were recorded with 2048 data points in the t2 domain and up to 1024 points in the t1 domain, with a 1s recovery delay.

Mass Spectrometry. High resolution and Accurate Mass spectra were recorded on a Bruker apex ultra FTMS and a Bruker microTOF-Q spectrometers using the electrospray technique.

UV-Vis Spectroscopy. Electronic spectra were recorded on a Varian Carry-50 Bio spectrophotometer. **Steady state fluorescence** spectra were recorded with a JASCO FP-8600 Spectrofluorometer apparatus. Quantum yields were determined using fluorescein (Φ = 0.95 in 0.1 M NaOH) as a reference compound. Time dependent experiments were recorded using the Edinburgh Instrument setup FL-900 using a nitrogen filled nanosecond flash lamp and the excitation wavelength of 350 nm, detected at the maximum of fluorescence and applying time correlated single photon counting (TCSPC) technique.

X-Ray Crystallography. X-Ray quality crystals were prepared by slow diffusion of methanol into the CH_2Cl_2 or $CHCl_3$ solution of proper compound. Data were collected at 100K on an Xcalibur PX-κ geometry diffractometer, with Cu Kα radiation (λ=1.5407) or Mo Kα (λ = 0.71073). Data were corrected for Lorentz and polarization effect. The structures were solved by intrinsic phases with SHELXT algorithm implemented into Shelx-2015 package.[1] The refinement of all structures was performed by full matrix least-squares method with using SHELXL algorithm from Shelx-2015 with anisotropic thermal parameters for the non-H atoms Scattering factors were those incorporated in SHELXT (2015).[1] The Olex[2] interface[2] has been used for handling (solving, refining, CIF preparing) all the data. For disordered solvent space in crystal cell the Masks subroutine in OlexSys (equivalent of SQEEZE in Platon) was used to remove contributions of: 10e for **2**, 25e for **2**-H_2, 15e for **2**-H_4, 4e for **3**, 359e for **4**. All those electrons come from solvent molecules (mostly chloroform) that have not been well defined.

Theoretical calculations. Geometry optimizations were carried out with the Gaussian 09[3] software package1 within unconstrained C1 symmetry, with starting coordinates derived from molecular

[1] Sheldrick, G.M. (2015). Acta Cryst. A71, 3-8; Sheldrick, G.M. (2015). Acta Cryst. C71, 3-8.

[2] Dolomanov, O.V., Bourhis, L.J., Gildea, R.J, Howard, J.A.K. & Puschmann, H. (2009), J. Appl. Cryst. 42, 339-341

[3] Gaussian 09, Revision E.01, M. J. Frisch ,G.W.Tucks, H. B. Schlege l, G. E. Scuseria ,M.A.Robb, J. R. Cheeseman, G. Scalmani, V. Barone,B. Mennucci, G. A. Petersson, H. Nakatsuji, M. Caricato, X. Li, H. P. Hratchian, A. F. Izmaylov ,J.Bloino ,G.Zheng ,J.L.Sonnenberg, M. Hada, M. Ehara, K. Toyota, R. Fukuda, J. Hasegawa, M. Ishida, T. Nakajima, Y. Honda, O.Kitao, H. Nakai, T. Vreven, J.A. Montgomery, Jr., J. E. Peralta,

mechanics or X-ray analysis. Becke's three-parameter exchange functional with the gradient-corrected correlation formula of Lee, Yang and Parr (DFT-B3LYP)[4] were used with the 6- 31G(d,p) basis set. Harmonic vibrational frequencies were calculated using analytical second derivatives as a verification of local minimum achievement with no negative frequencies observed. The structures were found to have converged to a minimum on the potential energy. Proton and carbon chemical shifts were calculated using the GIAO method and referenced to the absolute shielding of tetramethylsilane calculated at the same level of theory. The electronic spectra were simulated by means of time-dependent density functional theory (TD-DFT) using the Tamm-Dancoff approximation for 50 states. For TD calculations, the polarizable continuum model of solvation was used (PCM, standard dichloromethane parametrization). The electronic transitions and UV/Vis/NIR as well as CD spectra were analysed by means of the GaussSum program.[9] The transitions were convoluted by Gaussian curves with 2000 cm^{-1} half line width.

HPLC experiments. Chiral-resolving HPLC was performed by means of Hitachi LaChrom-7000 analytical chromatograph equipped with Chirex 3010 25/0.46 cm column filled with 5 µm silica gel covalently coated with L-valine and dinitroaniline as a stationary phase. Various mixtures of hexane with dichloromethane were used as mobile phases dependent on the polarity of separated compounds. The chromatographic profiles were collected by means of a Jasco flowcell attached to Jasco 1500 spectropolarimeter.

CD Experiments. Circular dichroic spectra were recorded in the region of 230-500 nm by means of Jasco 1500 spectropolarimeter for samples entrapped in a flowcell connected to the HPLC instrument. The concentrations of the samples were estimated on the basis of the absorption spectra recorded simultaneously with CD spectra.

F.Ogliaro, M. Bearpark, J. J. Heyd, E. Brothers, K. N. Kudin, V. N. Staroverov, R. Kobayashi, J. Normand,K. Raghavachari, A.Rendell, J. C. Burant, S. S. Iyengar,J.Tomasi, M. Cossi, N.Rega, J. M. Millam, M.Klene, J. E. Knox, J. B.Cross, V. Bakken, C. Adamo, J. Jaramillo, R. Gomperts, R. E. Stratmann, O. Yazyev, A.J.Austin, R. Cammi, C. Pomelli, J. W. Ochterski, R. L. Martin, K. Morokuma, V. G. Zakrzewski, G. A. Voth, P. Salvador, J.J.Dannenberg, S. Dapprich, A. D. Daniels, Farkas, J. B. Foresman, J. V. Ortiz, J. Cioslowski, D. J. Fox, Gaussian,Inc.,Wallingford,CT, 2009.

[4] a) C. T. Lee, W. T. Yang, R. G. Parr, Phys. Rev.B 1988, 37,785–789. b) A. D. Becke, Phys. Rev. A 1988, 38,3098–3100.

2. Synthesis.

Unless indicated differently solvents (CH_3NO_2, MeOH, $CHCl_3$, AcOEt, hexanes, 2-methylbutan-2-ol) were used without purification. CH_2Cl_2 was distilled over CaH_2. 1,4-dioxane was distilled over Na. THF, toluene and DMF were dried by passing through a silica column with an MBraun drying system. Purifications by column chromatography were performed on silica gel (Macherey-Nagel, Kieselgel 60, Mesh 70-210).

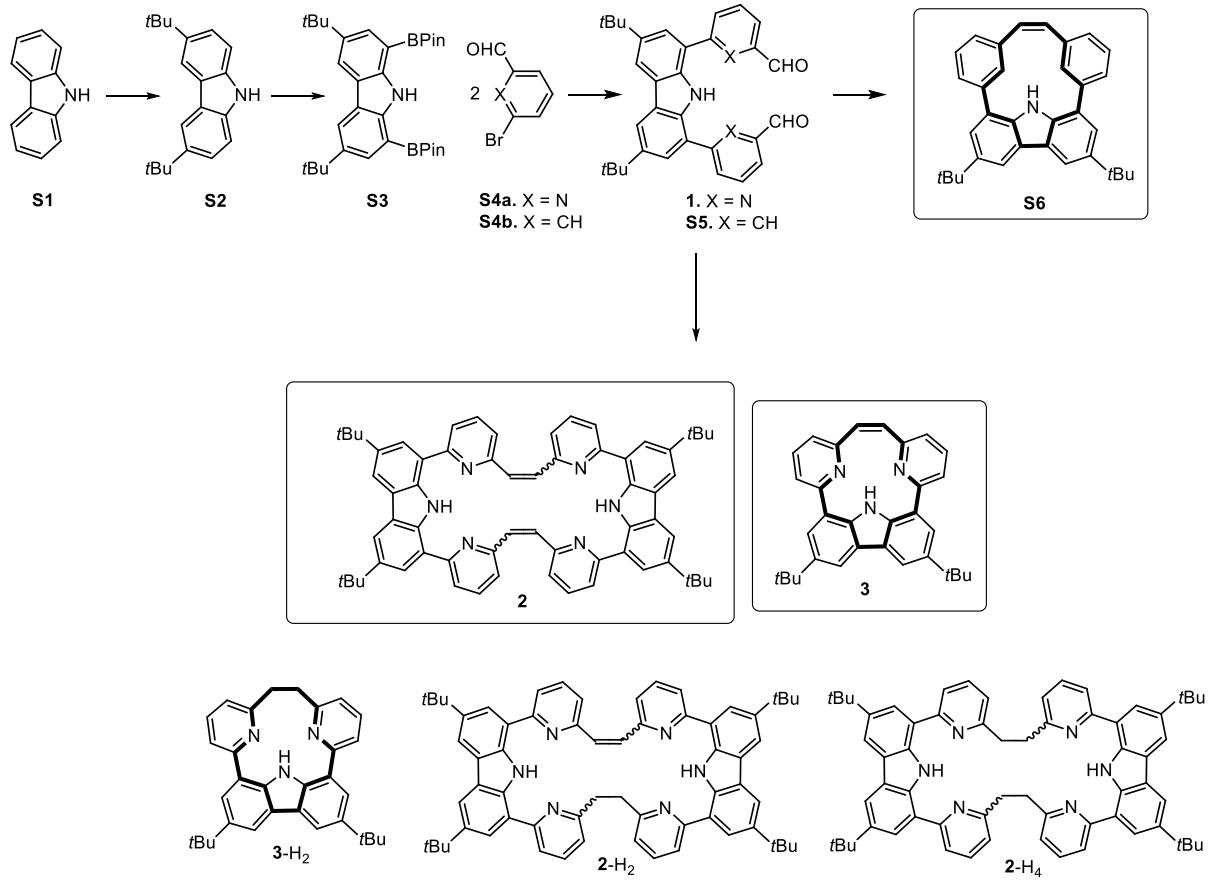

Scheme 1S. Synthetic approach.

3,6-di-*tert*-butyl-9*H*-carbazole S2: The synthesis was performed according to the procedure reported.[5] In the 500mL round bottom flask, equipped with magnetic stirring bar, carbazole (3.3g, 20mmol) and $ZnCl_2$ (8.1g, 60mmol) were suspended in nitromethane (150mL) and bubbled with argon for 15minutes. *Tert*-butyl chloride (6.5mL, 60mmol) was subsequently added slowly via syringe and the resulting mixture was stirred in room temperature for 6h. 110mL of water was added and the suspension was stirred for additional 30min. Then the mixture was extracted with CH_2Cl_2 (4x40mL), dried with $MgSO_4$ and evaporated to dryness to give crude product. Recrystallization from boiling

[5] Liu, Y., Nishiura, M., Wang, Y., Hou, Z., *J. Am. Chem. Soc.* **2006**, *128*, 5592

methanol gave 2.08g of product as white crystalline solid. The residue was concentrated yielding additional 0.75g portion of product. Yield: 50%. The ^{1}H NMR data were consistent with the literature.[2]

3,6-di-*tert*-butyl-1,8-bis(4,4,5,5-tetramethyl-1,3,2-dioxaborolan-2-yl)-9*H*-carbazole S3. The 100mL Schlenk vessel, equipped with magnetic stirring bar, was charged with 3,6-di-*tert*-butyl-*9H*-carbazole (1,114g, 4mmol), bis(pinacolato)diboron (2.03g, 8mmol, 2eq.), methoxy(cyclooctadiene) iridium(I) dimer $[Ir(COD)OMe]_2$ (0.04g, 0.06mmol, 0.015eq.) and 4,4'-di-tert-butyl-2,2'-bipirydyl (0.032g, 0.12mmol, 0.03eq.) and was evacuated and argonated several times. 30mL of dry 1,4-dioxane was added via syringe and the resulting mixture was refluxed for 24h and cooled to room temperature. The reaction mixture was evaporated in vacuo which was followed by recrystallization from methanol which gave 1.04g of the product as a white solid. Yield: 50% The ^{1}H NMR data were consistent with the literature.[6]

General procedure for Suzuki cross-coupling:

The 250mL two-neck round bottom flask, was charged with **3,6-di-*tert*-butyl-1,8-bis(4,4,5,5-tetramethyl-1,3,2-dioxaborolan-2-yl)-9*H*-carbazole S3** (1.06g, 2mmol), tetrakis(triphenylphosphine) palladium(0) (0.23g, 0.2mmol, 0.1eq.), potassium fluoride (0.47g, 8mmol, 4eq.), potassium carbonate (0.83g, 6mmol, 3eq.) and bromo-compound (4mmol, 2eq.). The mixture was dried under vacuum overnight. Then 70mL of dry toluene and 70mL of dry DMF were added via syringe. The mixture was then degassed by pump-thaw method and stirred in 110°C for 60-72h. After cooling to room temperature the solution was diluted with ethyl acetate and passed through pad of silica gel. After evaporation to dryness product was purified by column chromatography.

6,6'-(3,6-di-*tert*-butyl-9*H*-carbazole-1,8-diyl)di(pirydyl-2-carbaldehyde) 1: Reaction time: 72h. The product was purified by column chromatography on silica gel, eluted with CH_2Cl_2 as second fraction and recrystallized from CH_2Cl_2/MeOH to give yellow crystals. Yield: 48%. ^{1}H NMR (500MHz, $CDCl_3$) δ 12.23 (s, NH), 10.09 (s, 2H), 8.29 (m, 2H), 8.25 (m, 2H), 8.06 (m, 2H), 8.01 (m, 2H), 7.95 (m, 2H), 1.55 (s, 18H), ^{13}C NMR (151 MHz, $CDCl_3$) δ 192.5, 159.2, 152.1, 142.3, 138.0, 136.7, 125.1, 124.5, 122.6, 120.4, 119.8, 118.6, 34.9, 32.1, HRMS (ESI) *m/z* calcd for $C_{32}H_{31}N_3O_2$ $[M+H]^+$: 490.2489, found: 490.2479, UV/Vis (CH_2Cl_2, 298K, λ, log ε): 230 (5.23), 297 (4.64), 327 (4.59), 384 (4.39 M^{-1} cm^{-1}).

3,3'-(3,6-di-*tert*-butyl-9*H*-carbazole-1,8-diyl)di(benzaldehyde) S1: Reaction time: 72h. The product was purified by silica gel column chromatography, eluted with CH_2Cl_2/hexanes (2/1) as third fraction and recrystallized from CH_2Cl_2/MeOH to give white crystals. Yield: 50% ^{1}H NMR 600, $CDCl_3$) δ 10.13 (s, 2H), 8.24 (m, 2H), 8.19 (m, 2H), 8.19 (br. s, NH), 7.97 (m, 2H), 7.89 (m, 2H), 7.70 (m, 2H), 1.55 (s, 18H),

[6] Arnold, L., Norouzi-Arasi, H., Wagner, M., Enkelmann, V., Müllen, K., *Chem. Commun.* **2011**, *47*, 970-972

^{13}C NMR (151 MHz, $CDCl_3$) δ 192,1, 143,6, 140,5, 137,3, 135,7, 134,0, 130,0, 128,9, 128,8, 124,3, 123,9, 122,9, 116,5, 34,9, 32,1, HRMS (ESI) *m/z* calcd for $C_{34}H_{33}NO_2$ [2*M*+Na]$^+$: 997.4915, found: 997.4919, UV/Vis (CH_2Cl_2, 298K, λ, log ε): 234 (5.27), 298 (4.66), 358 (4.26 M^{-1} cm^{-1}).

General procedure for McMurry reaction.

In the two-neck round bottom flame-dried flask a zinc dust (0.13g, 2mmol, 10eq.) was dried under vacuum for 1h. Then 20mL of freshly distilled 1,4-dioxane from sodium (benzophenone indication of dryness) was added via syringe under the argon atmosphere, following by the addition of pyridine (0.8μL, 0.01mmol, 0.05eq.) and titanium tetrachloride (0.11mL, 1mmol, 5eq.). The mixture was refluxed for 1h and the solution of 0.2 mmol (1eq.) dialdehyde in dry 1,4-dioxane was added. The resulting solution was refluxed for additional 3h. Then the heating bath was removed, 20mL of saturated aqueous solution of NH_4Cl was added and the suspension was stirred for 20min and extracted with 3xCH_2Cl_2 and dried over Na_2SO_4. Further purification by column chromatography on silica gel gave pure product.

S5: Purification by column chromatography on silica gel, using CH_2Cl_2 as the eluent, gave product as first fraction. Recrystallization from CH_2Cl_2/MeOH gave pure compound. Yield: 27%. **^{1}H NMR (600MHz, $CDCl_3$)** δ 8.73 (s, NH), 8.04 (m, 2H), 7.92 (m, 2H), 7.57 (m, 2H), 7.56 (m, 2H), 7.47 (m, 2H), 7.23 (m, 2H), 6.91 (s, 2H), 1.51 (s, 18H), **^{13}C NMR (151 MHz, $CDCl_3$)** δ 142.9, 138.3, 138.0, 137.0, 132.4, 131.1, 129.6, 128.0, 127.0, 124.0, 123.1, 120.1, 116.8, 35.1, 32.2, **HRMS (ESI)** *m/z* calcd for $C_{34}H_{33}N$ [*M*+Na]$^+$: 478.2499, found: 478.2511, **UV/Vis (CH_2Cl_2, 298K, λ, log ε)**: 237 (4.70), 304 (4.34), 358 (3.98 M^{-1} cm^{-1}).

3: The crude mixture was passed through a short silica plug with CH_2Cl_2 as the eluent. The obtained pale yellow mixture was separated on size-exclusion column (BioBeads-S-X1) to give two fractions. The first fraction contained dimeric molecule **2** (yield 10%) and the second one triphyrin(2.1.1)-like **3** (yield 35%).

2: **^{1}H NMR (600MHz, $CDCl_3$)** δ 12.84 (s, 2xNH), 8.27 (d, ^4J=1.6 Hz, 4H), 7.95 (d, ^4J=1.6 Hz, 4H), 7.80 (d, ^3J=7.9 Hz, 4H), 7.65 (s, 4H), 7.52 (t, ^3J=7.9 Hz, 4H), 6.41 (d, ^3J=7.6 Hz, 4H), 1.55 (s, 36H), **^{13}C NMR (151 MHz, $CDCl_3$)** δ 158.1, 154.1, 141.8, 137.1, 137.0, 131.2, 124.2, 121.9, 121.8, 121.2, 119.5, 117.8, 34.9, 32.2; **UV/Vis (CH_2Cl_2, 298K, λ, log ε):** 320 (4.52), 373 (sh), 390 (4.30 M^{-1} cm^{-1}). **HRMS** (ESI) *m/z* calcd for $C_{64}H_{62}N_6$ [*M+H*]$^+$: 915.5109, found: 915.5071.

3: ^{1}H NMR (600MHz, $CDCl_3$) δ 17.78 (s, NH), 8.18 (d, ^4J=1.4 Hz, 2H), 7.97 (d, ^4J=1.4 Hz, 2H), 7.93 (d, ^3J=8.0 Hz, 2H), 7.75 (t, ^3J=8.0 Hz, 2H), 7.19 d, ^4J=7.7 Hz, 2H), 6.54 (s, 2H), 1.51 (s, 18H); **^{13}C NMR (151 MHz, $CDCl_3$)** δ 157.6, 154.5, 141.1, 138.6, 137.0, 132.4, 126.1, 123.2, 119.5, 119.3, 118.2, 117.5, 35.1,

32.4; **UV/Vis (CH_2Cl_2, 298K, λ, log ε):** 248 (4.68), 313 (4.47), 419 (4.03 M^{-1} cm^{-1}). **HRMS** (ESI) *m/z* calcd for $C_{32}H_{31}N_3$ $[M]^+$: 457.2513, found: 457.2506.

Depending on the quality of reagents ($TiCl_4$ and dryness of dioxane) we have observed a formation of structures containing saturated bonds: monomeric (**3**-H_2) and dimeric (**2**-H_2 and **2**-H_4). While such mixture has been isolated from the reaction mixture the separation with size-exclusion column gave two fractions F1 and F2 containing **2**, **2**-H_2 and **2**-H_4 and **3**, **3**-H_2 respectively. All of them were characterized in details (see below) after purification that has been achieved with a support from HPLC techniques on regular silica column with different mixtures of hexane and dichloromethane as a moving phase depending on the polarity of analysed mixture.

2-H_2: **^{1}H NMR (600MHz, $CDCl_3$)** δ 12.32 (s, 2xNH), 8.26 (d, ^4J=1.7 Hz, 2H), 8.24 (d, ^4J=1.7 Hz, 2H), 7.93 (d, ^4J=1.7 Hz, 2H), 7.91 (d, ^4J=1.7 Hz, 2H), 7.80 (d, ^3J=8.4 Hz, 2H), 7.76 (d, ^3J=7.7 Hz, 2H), 7.68 (s, 2H), 7.55 (t, ^3J=7.7 Hz, 2H), 7.49 (d, ^3J=7.7 Hz, 2H), 6.51 (d, ^3J=7.7 Hz, 2H), 6.48 (d, ^3J=7.7 Hz, 2H), 3.73 (bs, 3H), 3.10 (bs, 2H), 1.55 (s, 18H), 1.54 (s, 18H); **^{13}C NMR (partial data, 151 MHz, $CDCl_3$)** δ 137.3, 136.5, 131.5 (CH=CHbridge), 122.3, 121.9 (carbazole), 121.9, 121.1 (pyridine), 119.9, 117.9, 117.8, 117.3 (carbazole), 32.2; **UV/Vis (CH_2Cl_2, 298K, λ, log ε):** 297 , 320 (4.54), 370 (sh), 387 (4.30 M^{-1} cm^{-1}). **HRMS** (ESI) *m/z* calcd for $C_{64}H_{64}N_6$ $[M+1]^+$: 917.5265, found: 917.5244.

2-H_4: **^{1}H NMR (600MHz, $CDCl_3$)** δ 11.88 (s, 2xNH), 8.25 (d, ^4J=1.6 Hz, 4H), 7.90 (d, ^4J=1.6 Hz, 4H), 7.77 (d, ^3J=7.7 Hz, 4H), 7.47 (t, ^3J=7.7 Hz, 4H), 6.54 (d, ^4J=7.6 Hz, 4H), 3.41 (s, 8H), 1.54 (s, 3H); **^{13}C NMR (151 MHz, $CDCl_3$)** δ 160.2, 157.8, 141.8, 136.7, 136.6, 124.3, 122.5, 121.8, 121.0, 118.2, 117.3, 34.8, 34.4, 32.2, **UV/Vis (CH_2Cl_2, 298K, λ, log ε):** 302 (4.65), 322 (4.15), 384 (4.30 M^{-1} cm^{-1}). **HRMS (ESI)** *m/z* calcd for $C_{64}H_{66}N_6$ $[M+1]^+$: 919.5422, found: 919.5386.

3-H_2: **^{1}H NMR (600MHz, $CDCl_3$)**; 16.32 (s, NH), 8.22 (d, ^4J=1.4 Hz, 2H), 8.03 (d, ^4J=1.4 Hz, 2H), 7.91 (d, ^3J=7.9 Hz, 2H), 7.75 (t, ^3J=7.7 Hz, 2H), 7.12 (d, ^3J=7.7 Hz, 2H), 3.35 (s, 4H), 1.52 (s, 18H); **^{13}C NMR (151 MHz, $CDCl_3$)** δ 160.9, 157.2, 140.9, 138.2, 137.1, 123.4, 120.0, 119.2, 119.0, 118.5, 117.1, 36.8, 35.1, 32.4; **UV/Vis (CH_2Cl_2, 298K, λ, log ε):** 302 (4.38), 361 (4.31), 408 (4.28 M^{-1} cm^{-1}). **HRMS (ESI)** ***m/z*** calcd for $C_{32}H_{33}N_3$ $[2M+Na]^+$: 941.5241, found: 941.52433.

Photocyclisation of 2: In an inert atmosphere 4 mg (4.3 mmol) of **2** was dissolved in 1 mL of dry deoxygenated $CHCl_3$ and the resulting solution was irradiated with a UV lamp (365 nm) for 72h. After that time the solution was evaporated and the residue re-dissolved in freshly distilled CH_2Cl_2 and precipitated with MeOH to quantitatively give **4**. **^{1}H NMR (600MHz, $CDCl_3$)** δ 14.67 (s, 2xNH), 8.32 (d, ^4J=1.6 Hz, 4H), 8.23 (d, ^4J=1.6 Hz, 4H), 8.03 (d, ^3J=8.7 Hz, 4H), 7.55 (d, ^3J=7.7 Hz, 4H), 6.80 (d, ^3J=7.5 Hz, 4H), 4.98 (s, 4H), 1.57 (s, 36H); **^{13}C NMR (151 MHz, $CDCl_3$)** δ 160.8, 157.8, 141.4, 137.5, 136.4, 124.3, 120.6, 120.4, 119.6, 118.2, 117.2, 51.2, 35.0, 32.1; **UV/Vis (CH_2Cl_2, 298K, λ, log ε):** 316 , 353(4.71), 379 (4.30), 397 (4.38 M^{-1} cm^{-1}). **HRMS** (ESI) *m/z* calcd for $C_{64}H_{62}N_6$ $[M+H]^+$: 915.5109, found: 915.5088.

The ^{1}H NMR monitored conversion (Figure S1) was performed on the sample prepared in the same way as the above description but with $CDCl_3$ used as a solvent. The amounts of sample and solvent were reduced by half (2 mg of **5** in 500 ul of $CDCl_3$).

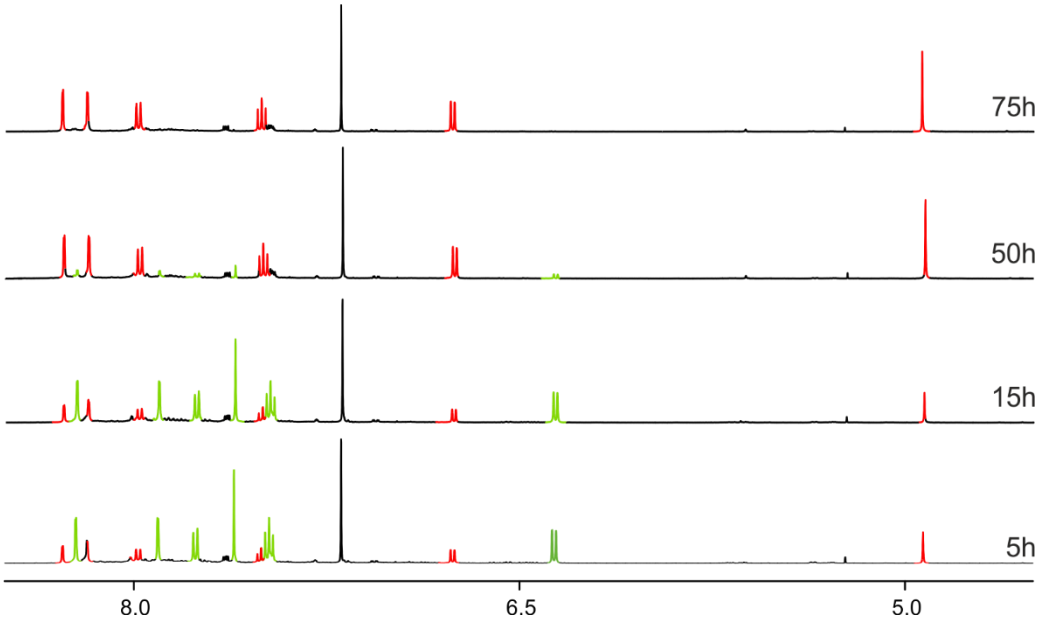

Figure S1. ^{1}H NMR monitored conversion of **2** to **4** ($CDCl_3$, 600 MHz, 300K). The forming product's **4**) resonances are presented in red while the disappearing lines of **2** in green.

3. NMR spectra.

3.1. NMR spectra of 1.

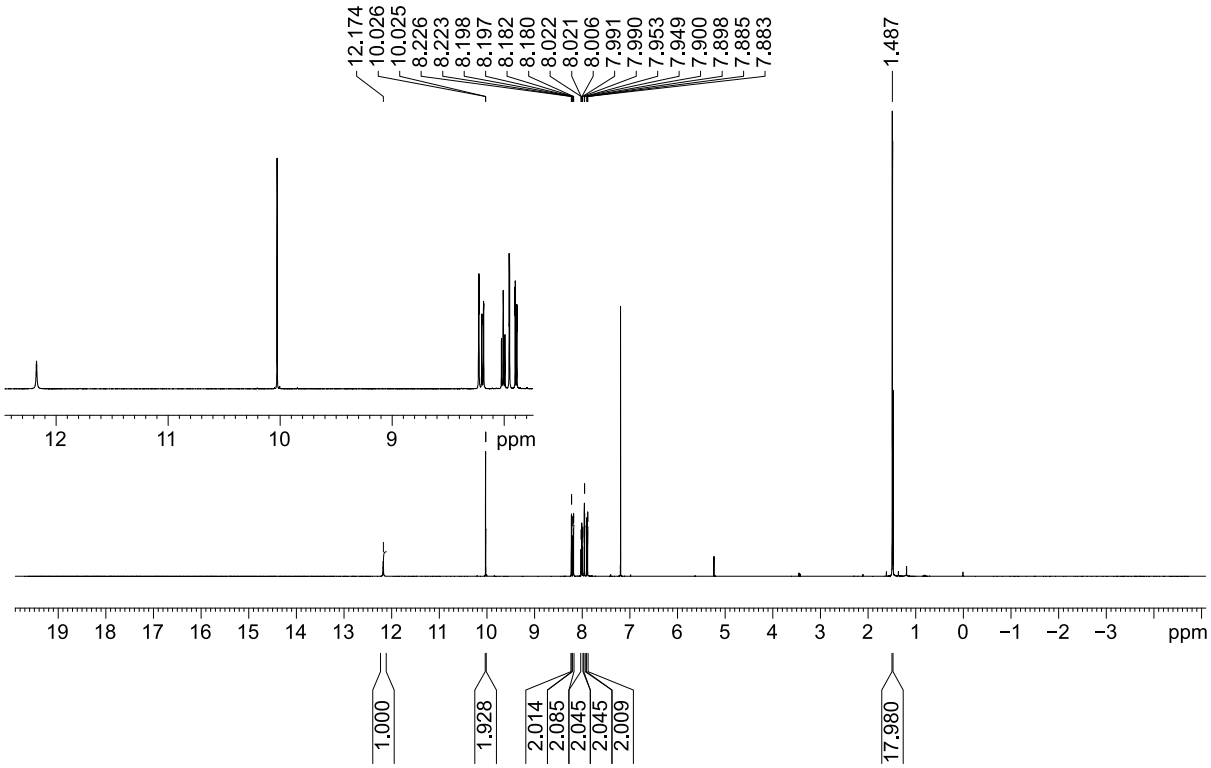

Figure S2. ^{1}H NMR spectrum of **3a (600 MHz, $CDCl_3$, 300K)**

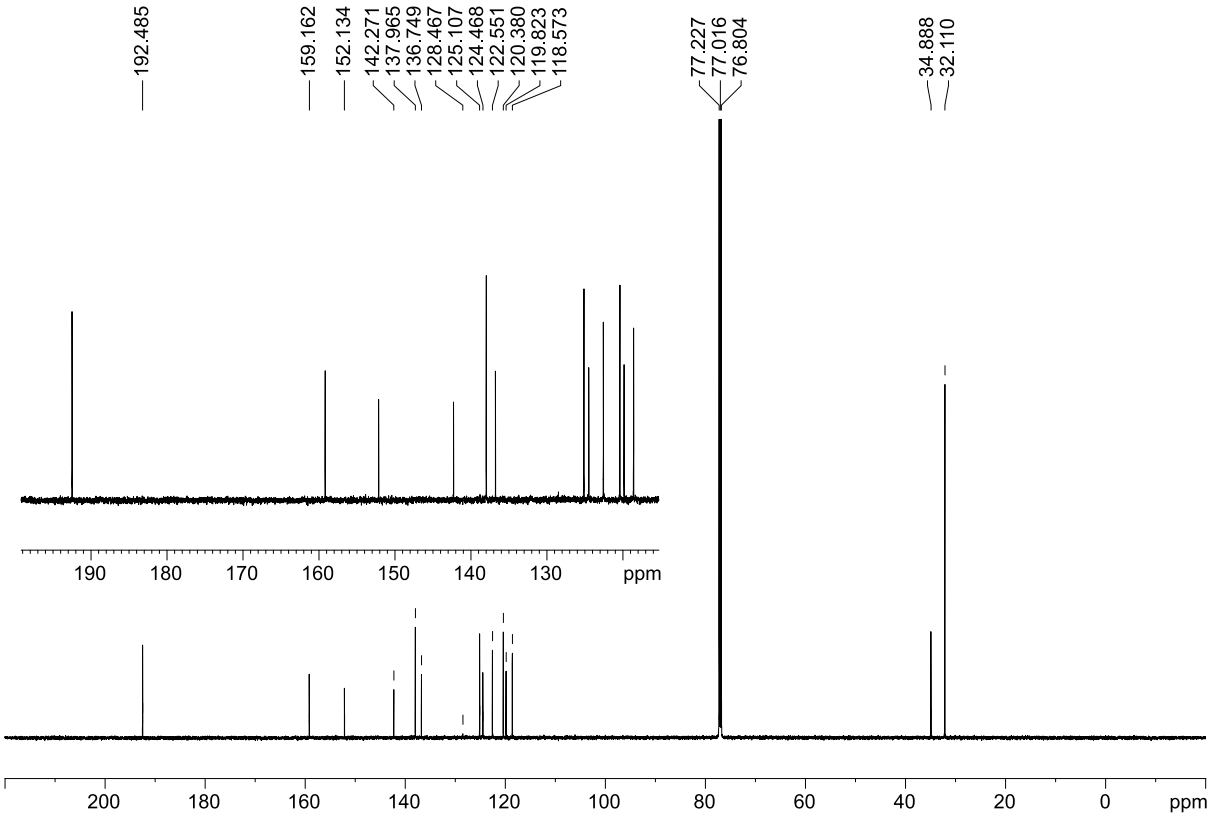

Figure S3: ^{13}C NMR spectrum of **1 (151 MHz, $CDCl_3$, 300K)**

3.2. NMR spectra of S5.

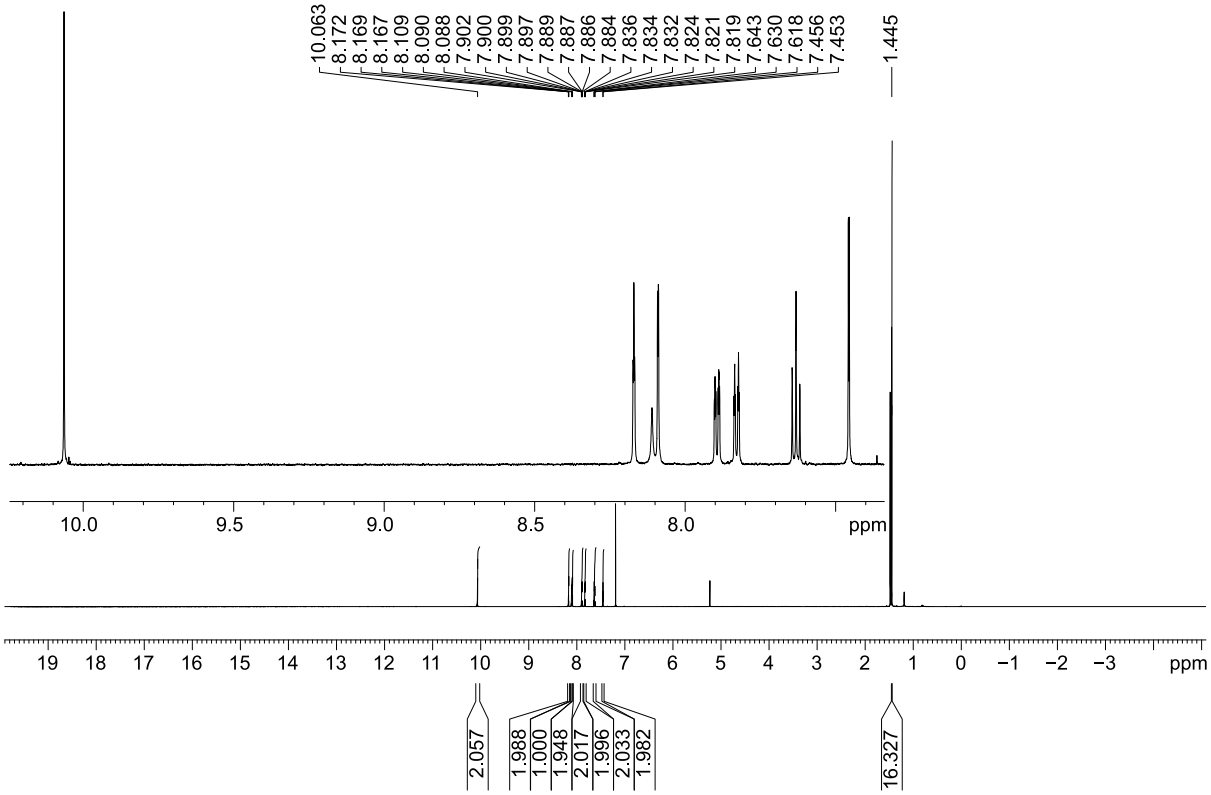

Figure S4. ^{1}H NMR spectrum of **S5 (600 MHz, $CDCl_3$, 300K)**

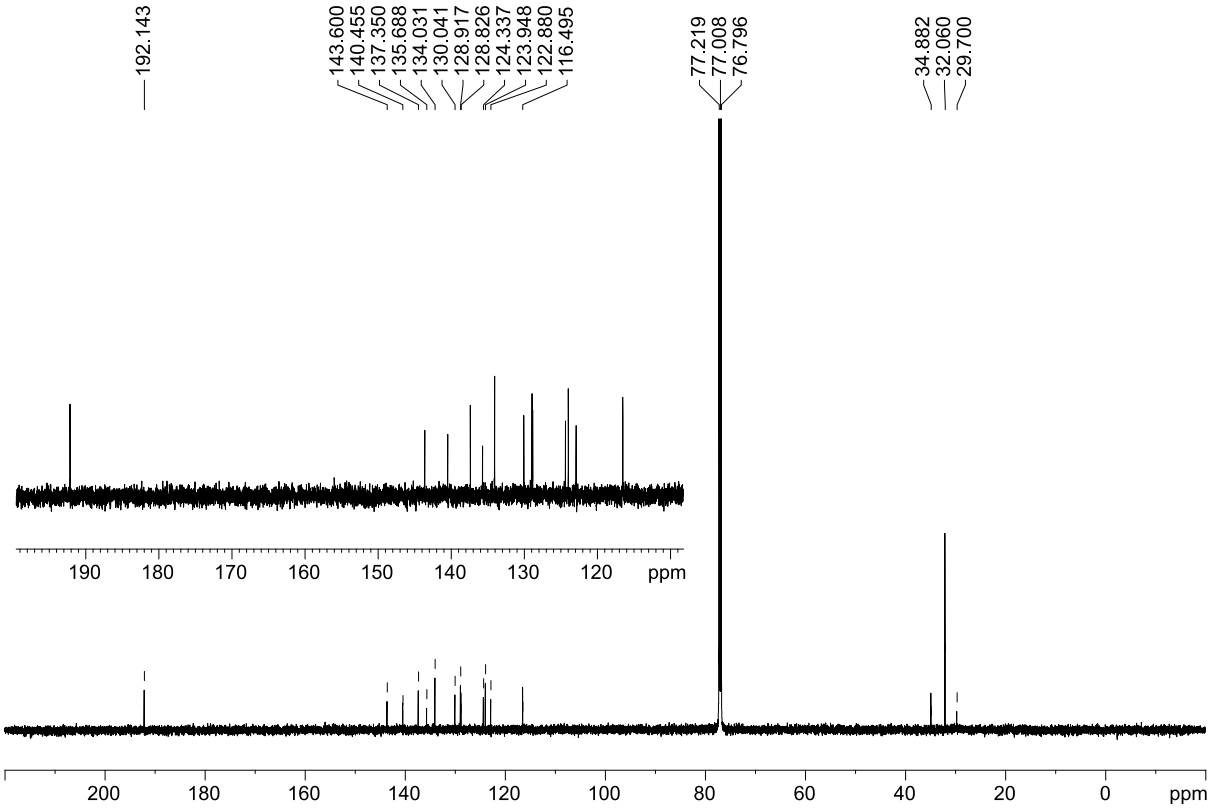

Figure S5. ^{13}C NMR spectrum of **S5 (151 MHz, $CDCl_3$, 300K)**

3.3. NMR spectra of 3.

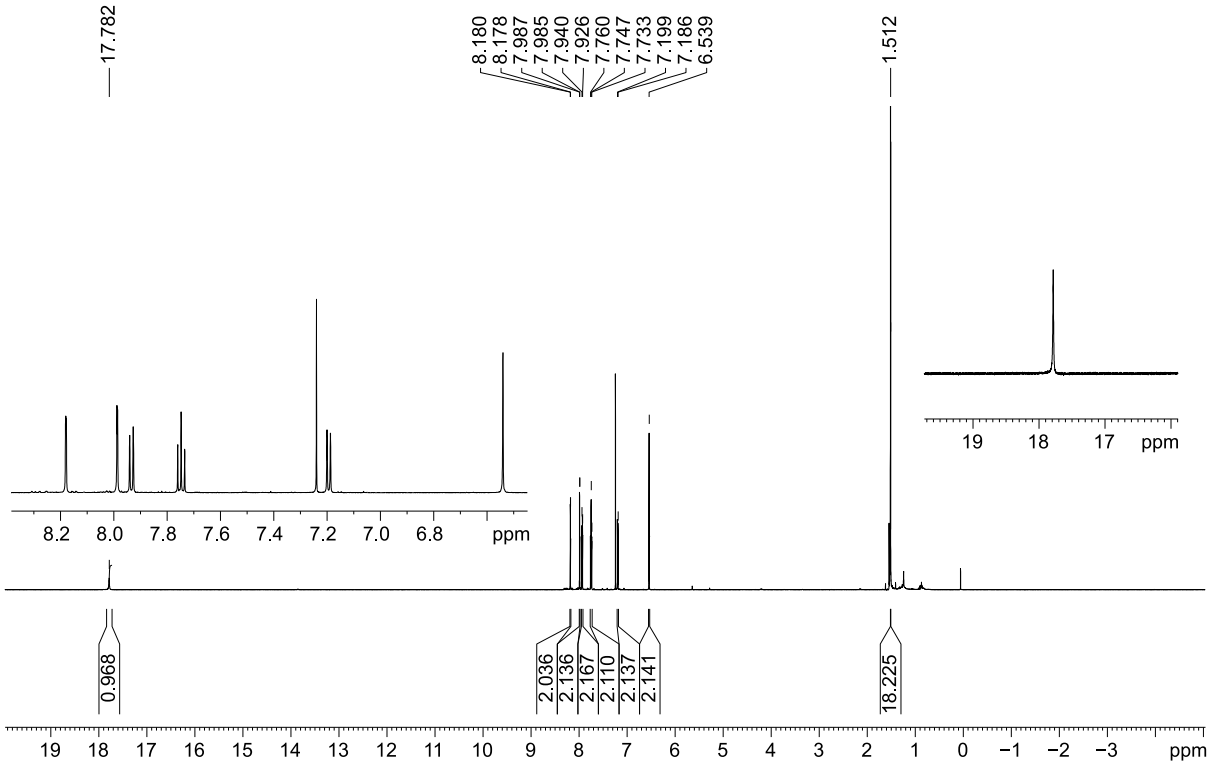

Figure S6. ^{1}H NMR spectrum of **3 (600 MHz, $CDCl_3$, 300K)**

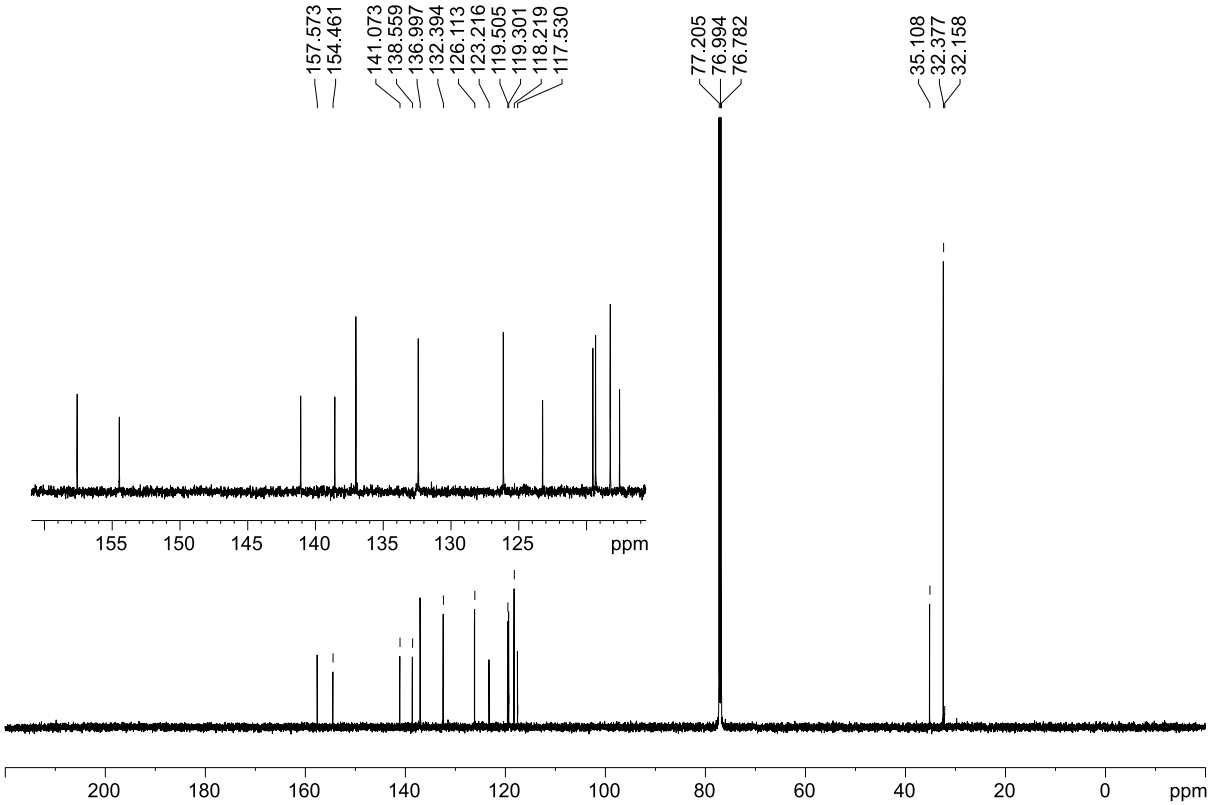

Figure S7. ^{13}C NMR spectrum of **3 (151 MHz, $CDCl_3$, 300K)**

3.4. NMR spectra of S6.

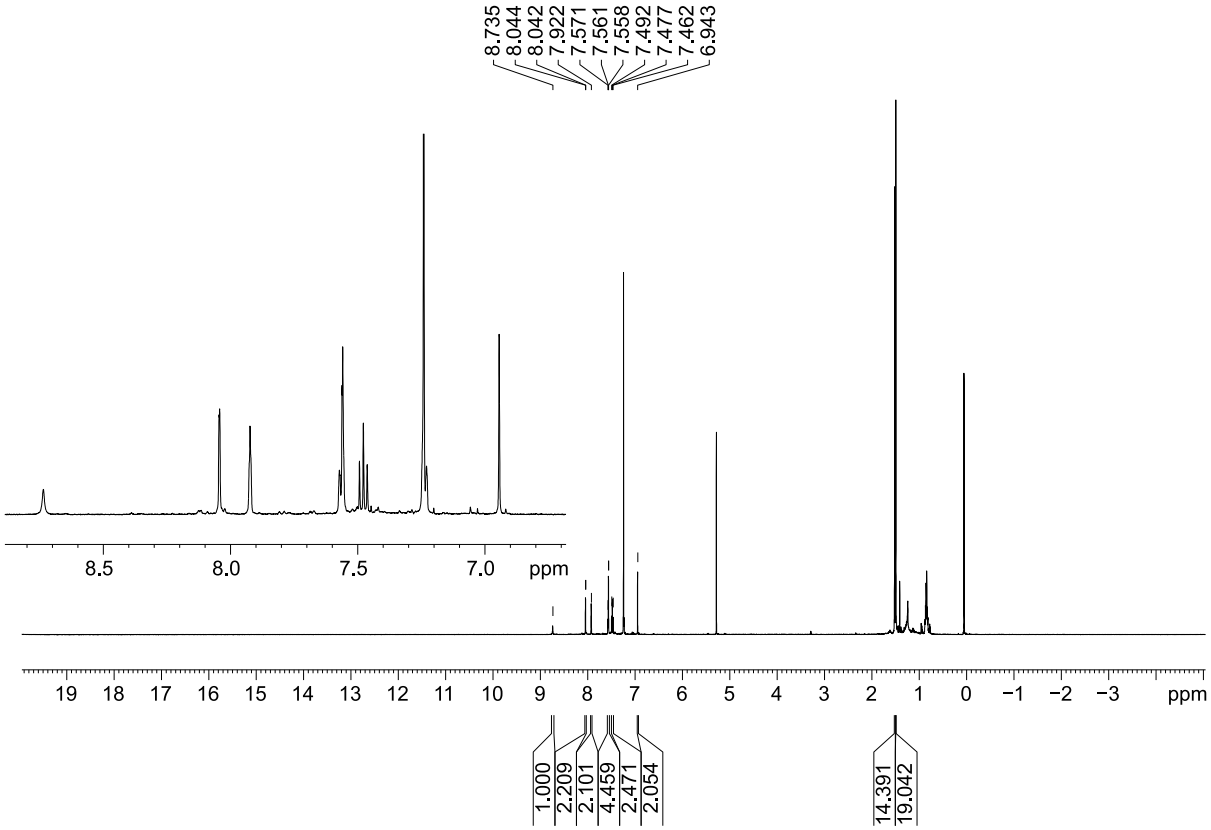

Figure S8: ^{13}C NMR spectrum of **S6 (600 MHz, $CDCl_3$, 300K)**

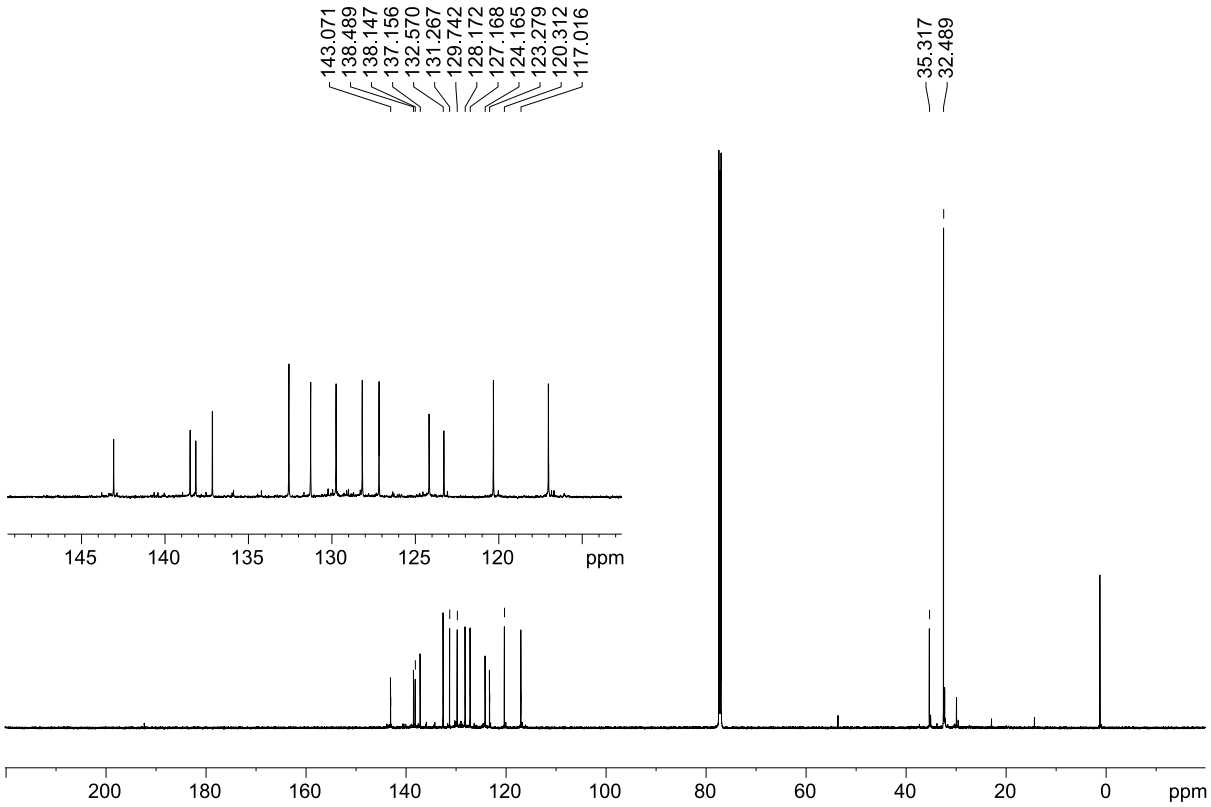

Figure S9: ^{13}C NMR spectrum of **S6 (151 MHz, $CDCl_3$, 300K)**

3.5. NMR spectra of 2.

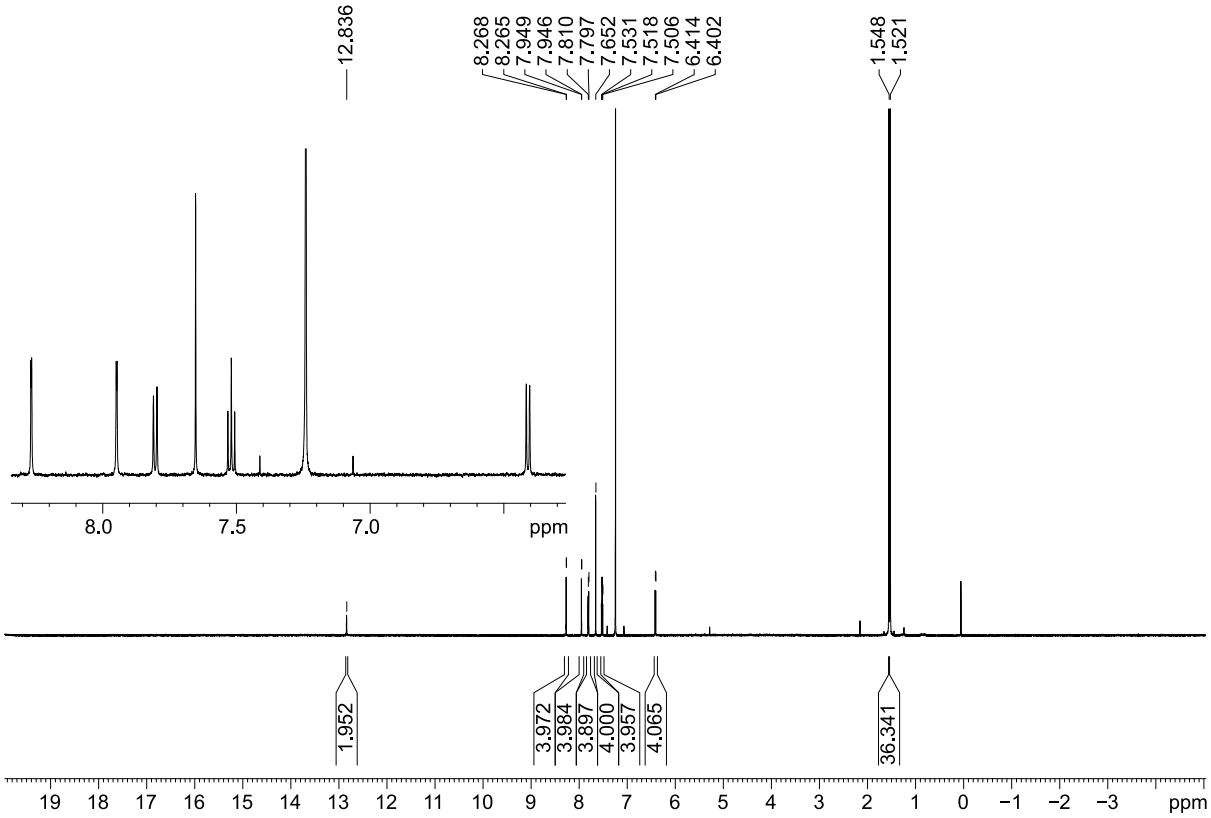

Figure S10. ^{1}H NMR spectrum of **2** ($CDCl_3$, 600MHz, 300 K).

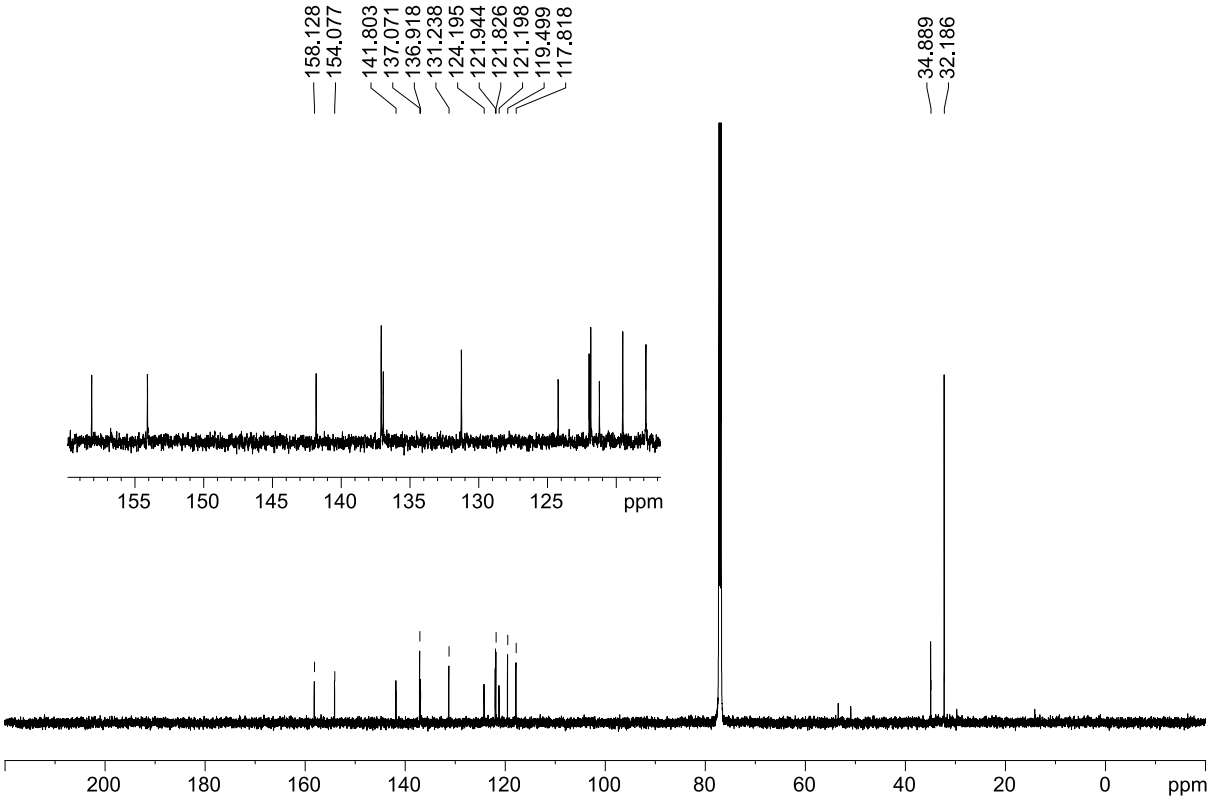

Figure S11. ^{13}C NMR spectrum of **2** ($CDCl_3$, 150MHz, 300 K).

3.6. NMR spectra of 4.

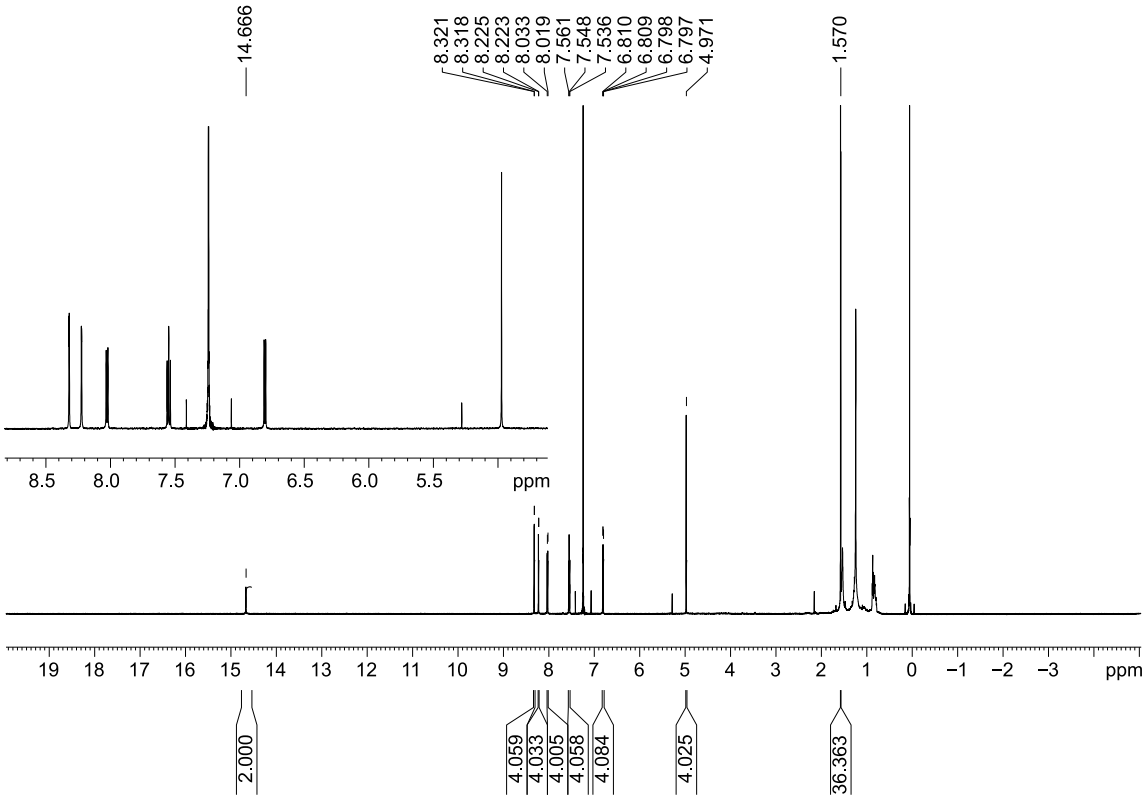

Figure S12. ^{1}H NMR spectrum of **4** ($CDCl_3$, 600 MHz, 300K)

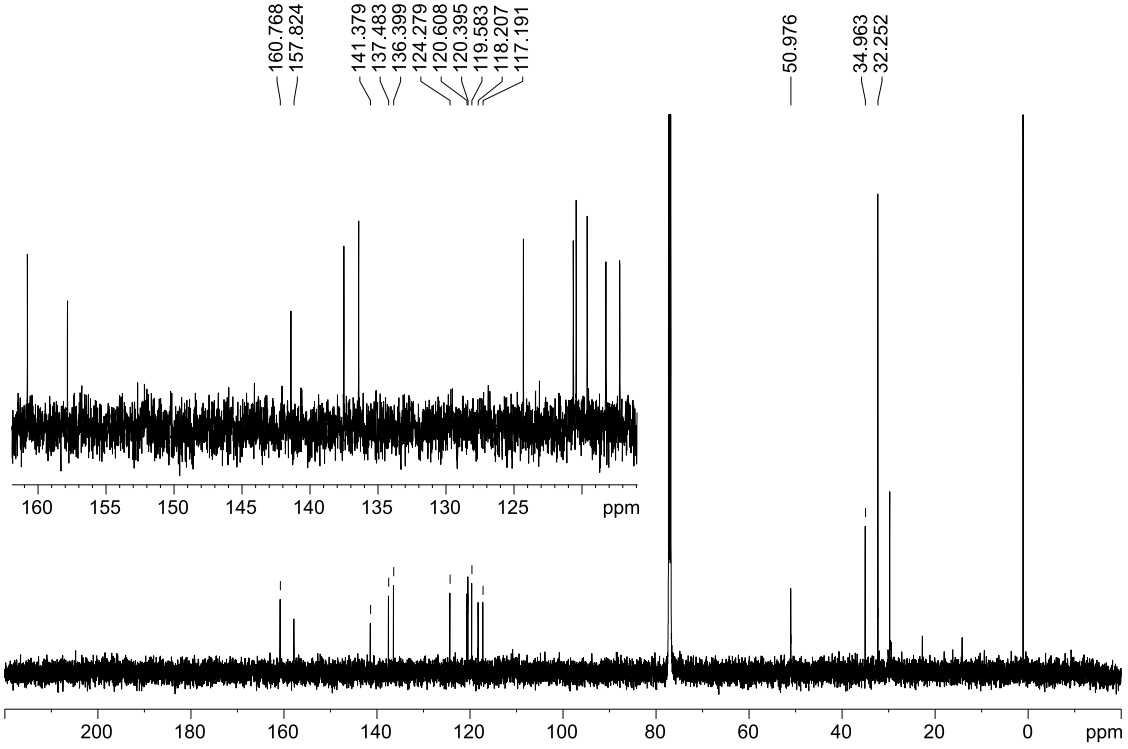

Figure S13. ^{13}C NMR spectrum of **4** ($CDCl_3$, 150MHz, 300 K).

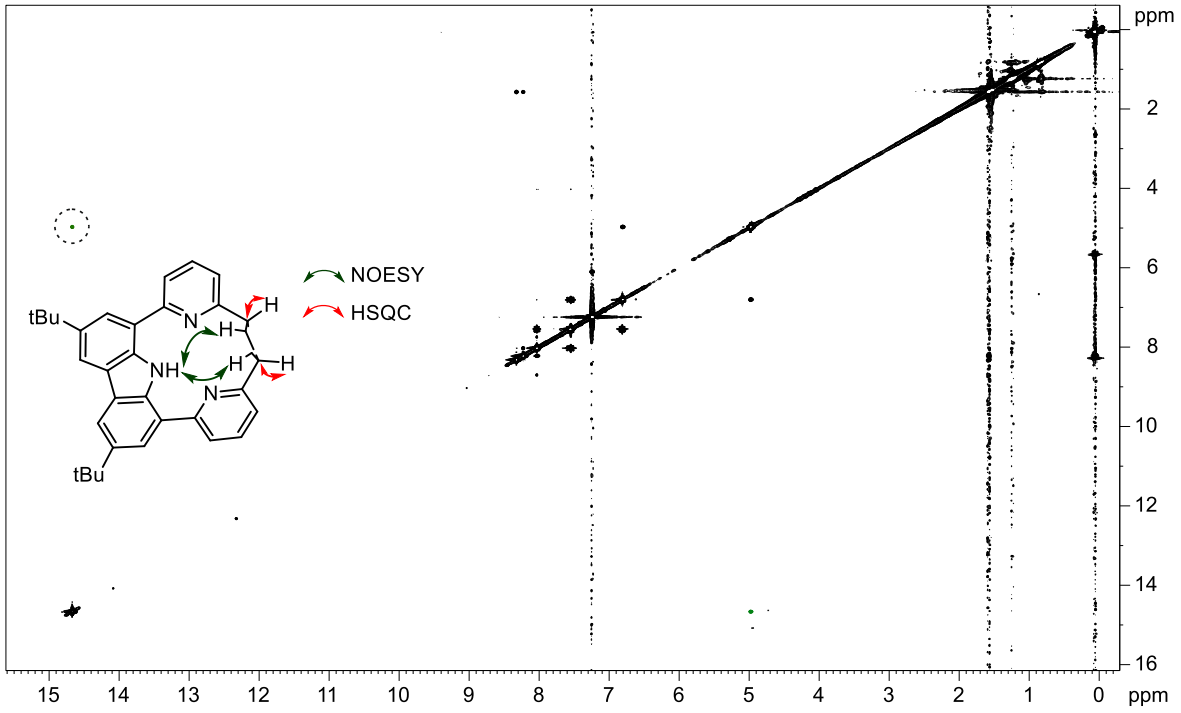

Figure S14. NOESY experiment for **4** ($CDCl_3$, 600MHz, 300K; a crucial NOE contact marked in green).

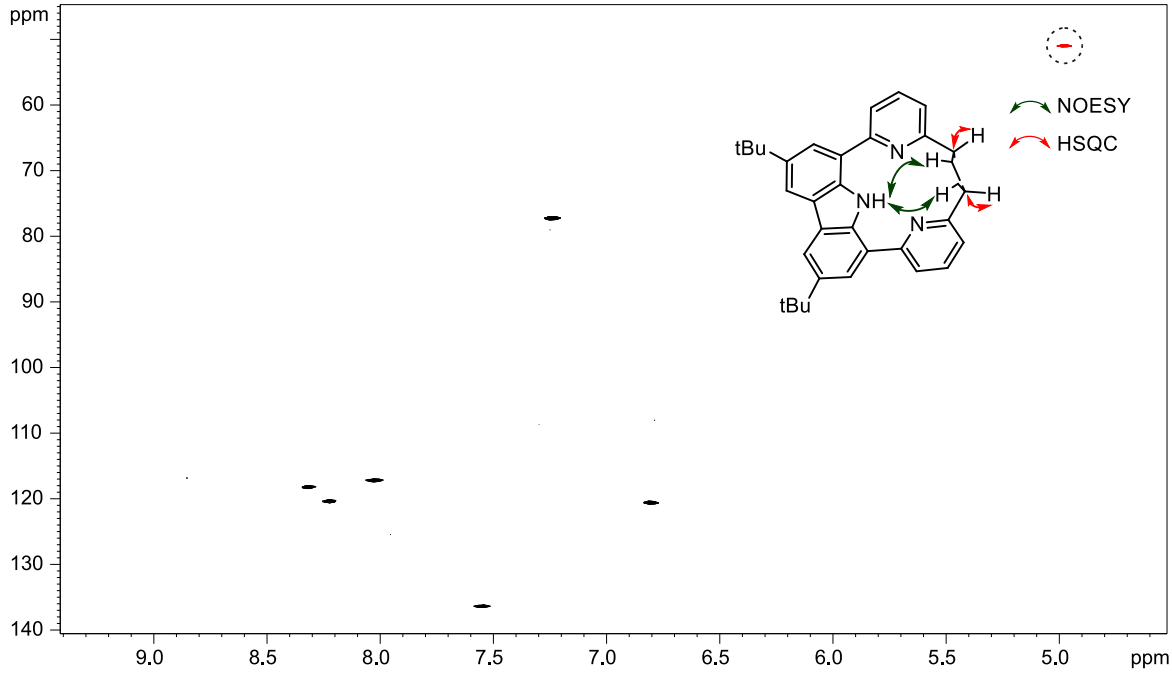

Figure S15. HSQC experiment for **4** ($CDCl_3$, 600MHz, 300K; a crucial correlation marked in red)

3.7. NMR spectra of 3-H_2.

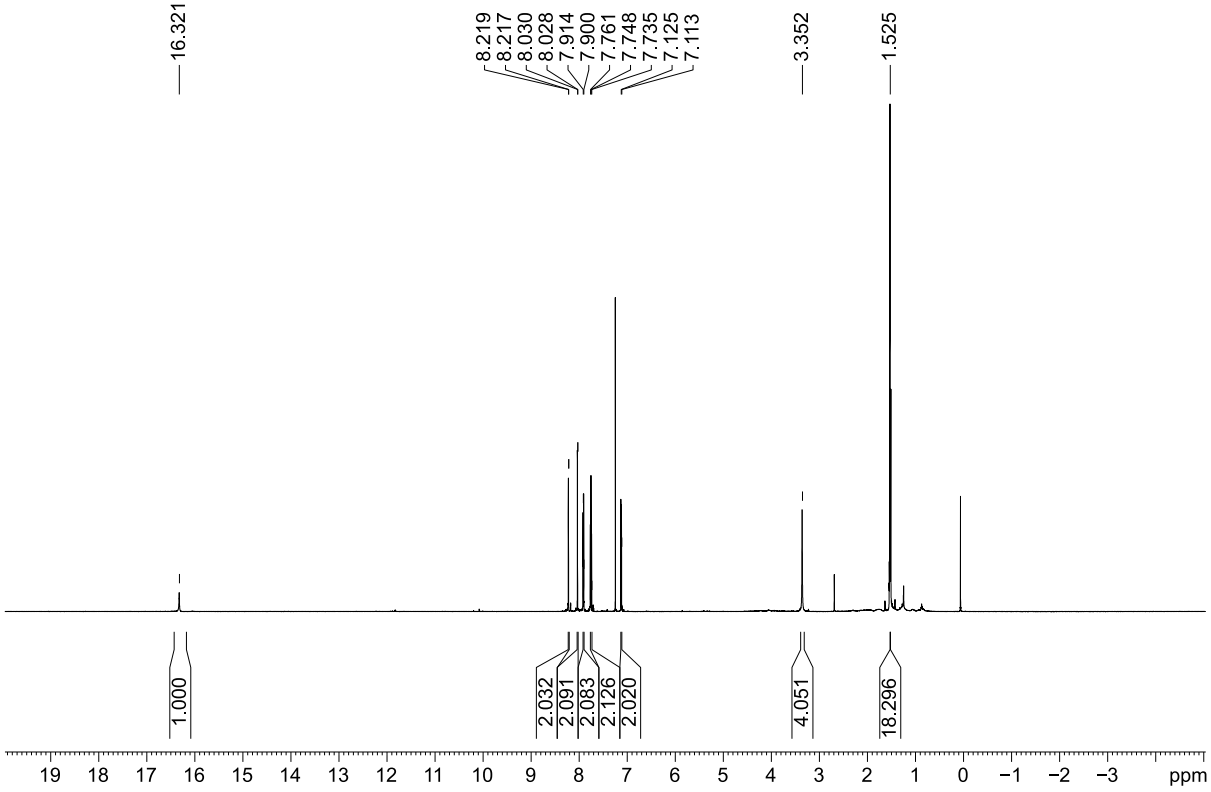

Figure S16. ^{1}H NMR spectrum of **3-H_2 (600 MHz, $CDCl_3$, 300K)**

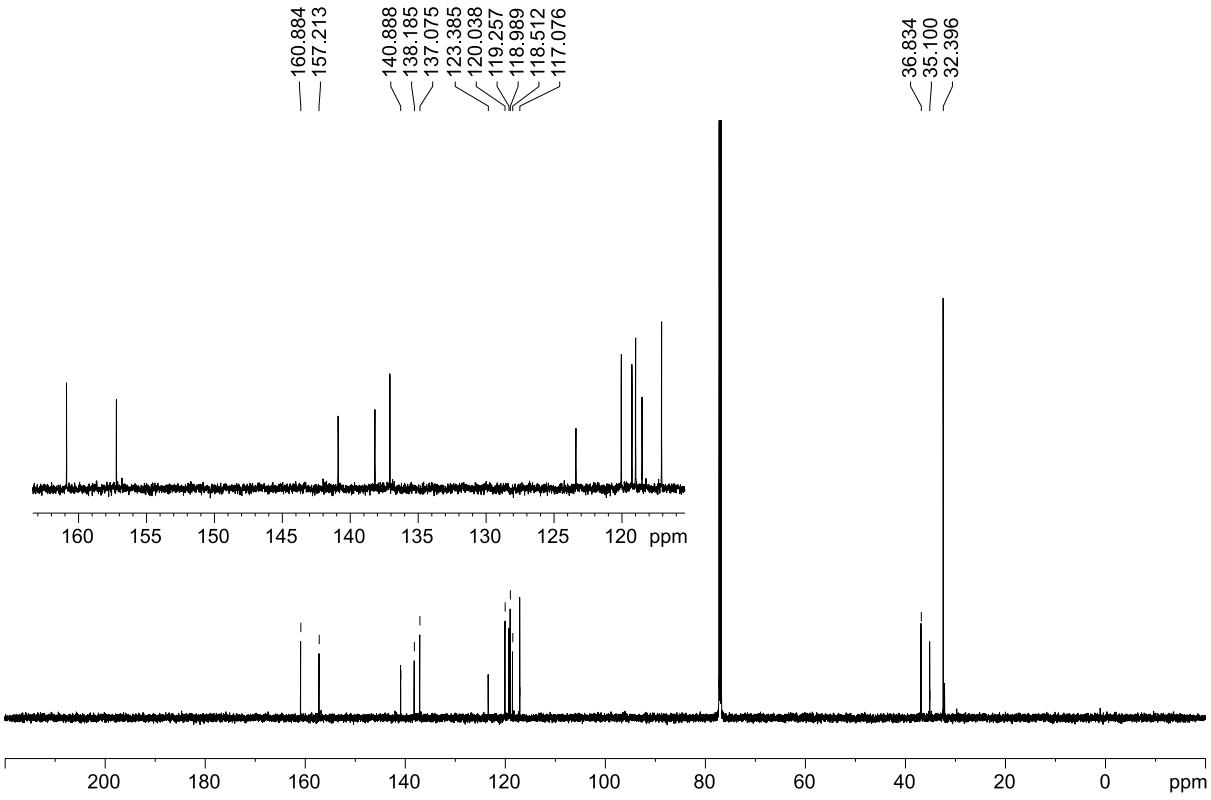

Figure S17. ^{13}C NMR spectrum of **3-H_2 (151 MHz, $CDCl_3$, 300K)**

3.8. NMR spectra of **2-H$_2$**.

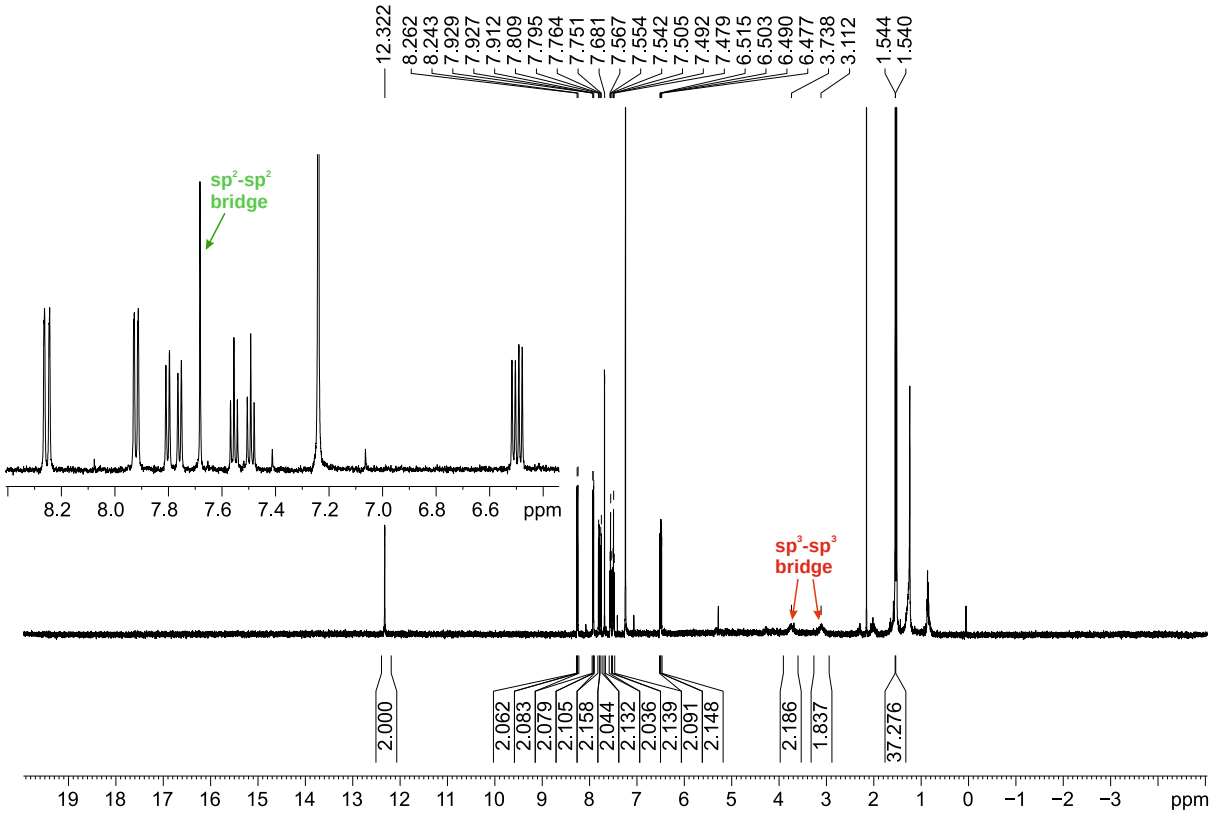

Figure S18. ^{1}H NMR spectrum of **2-H$_2$** ($CDCl_3$, 600 MHz, 300K).

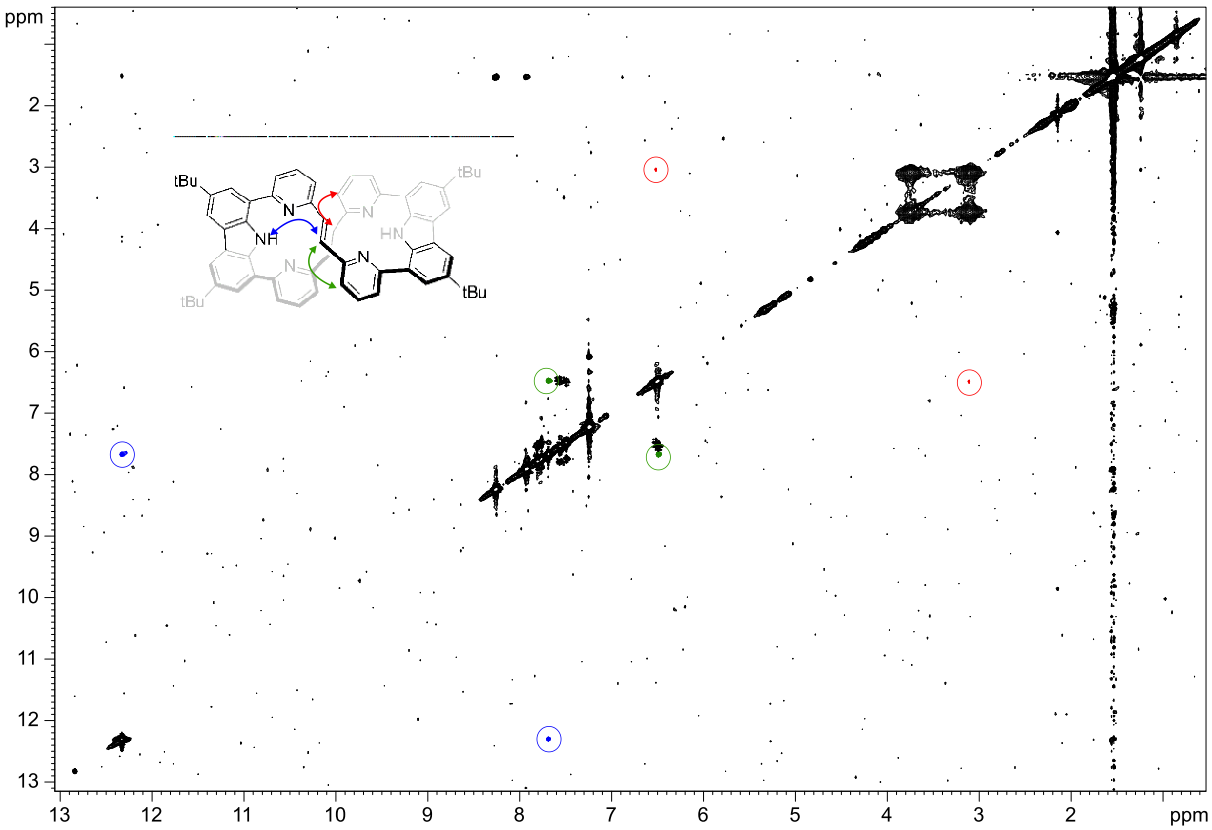

Figure S19. NOESY experiment for **2H$_2$** ($CDCl_3$, 600MHz, 300K).

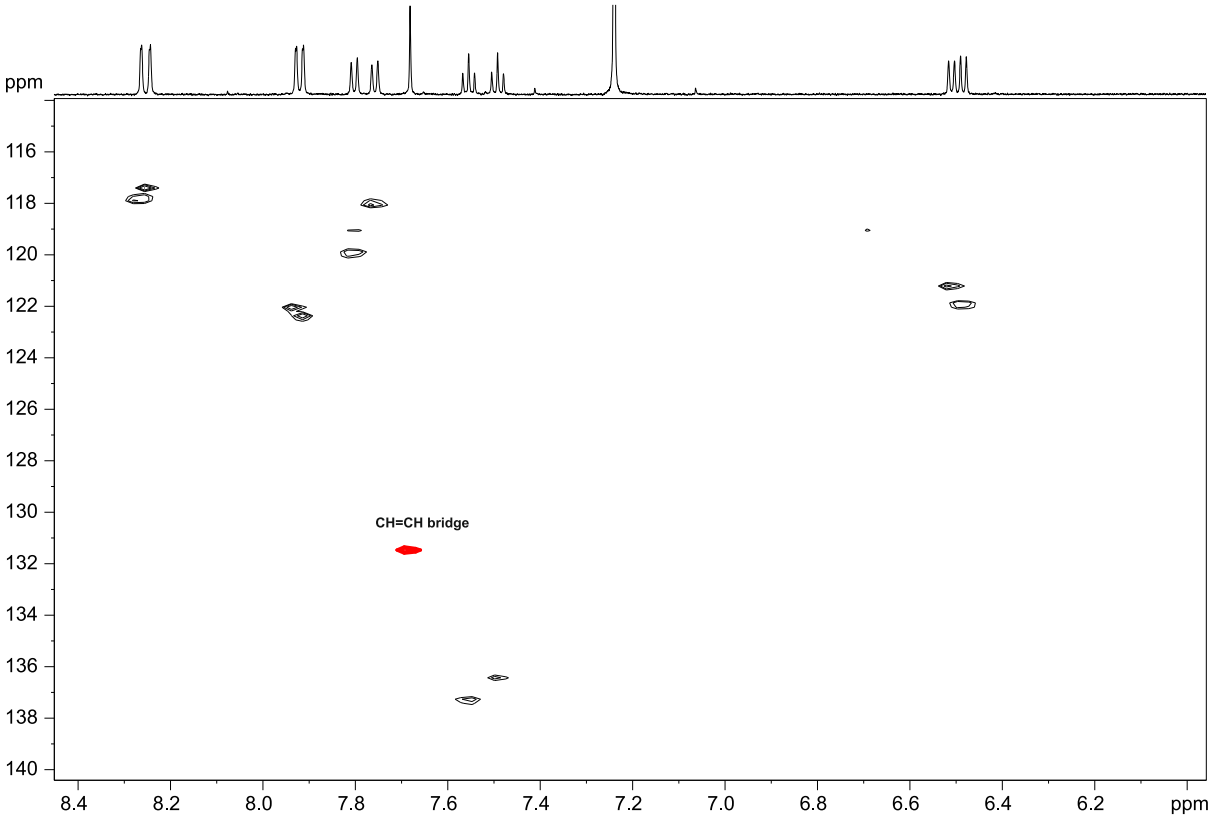

Figure S20. HSQC experiment for **2-H_2** ($CDCl_3$, 600 MHz, 300K).

3.9. NMR spectra of **2-H$_4$**.

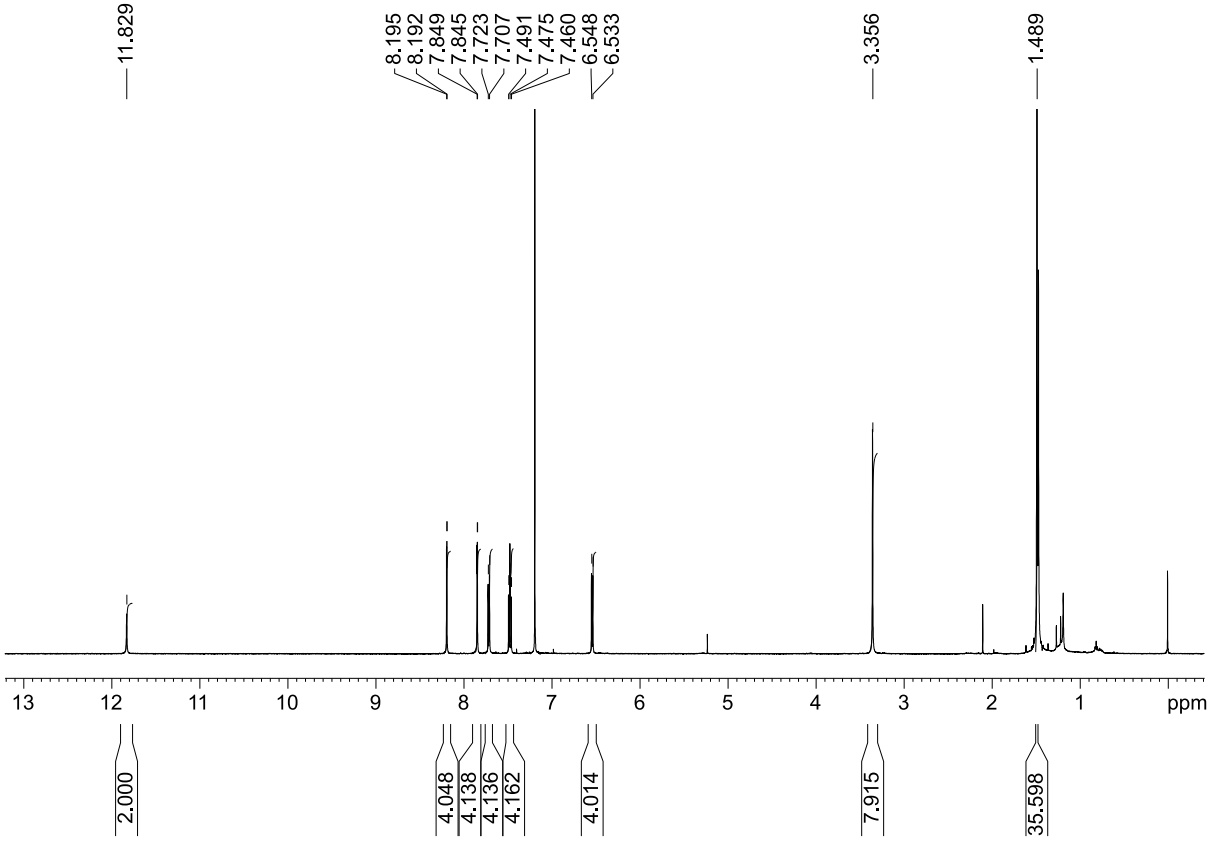

Figure S21. ^{1}H NMR spectrum of **2-H$_4$ (600 MHz, CDCl$_3$, 300K)**

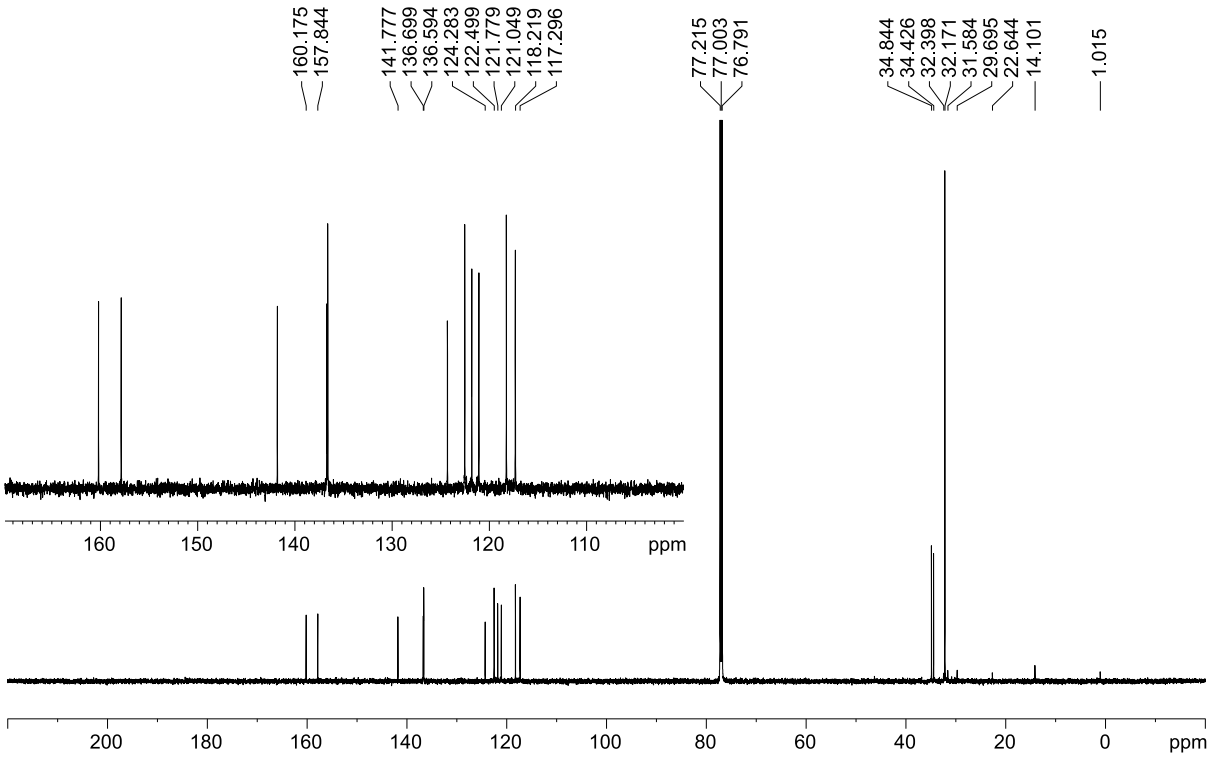

Figure 22. ^{13}C NMR spectrum of **2-H$_4$ (151 MHz, CDCl$_3$, 300K)**

4. Mass Spectra

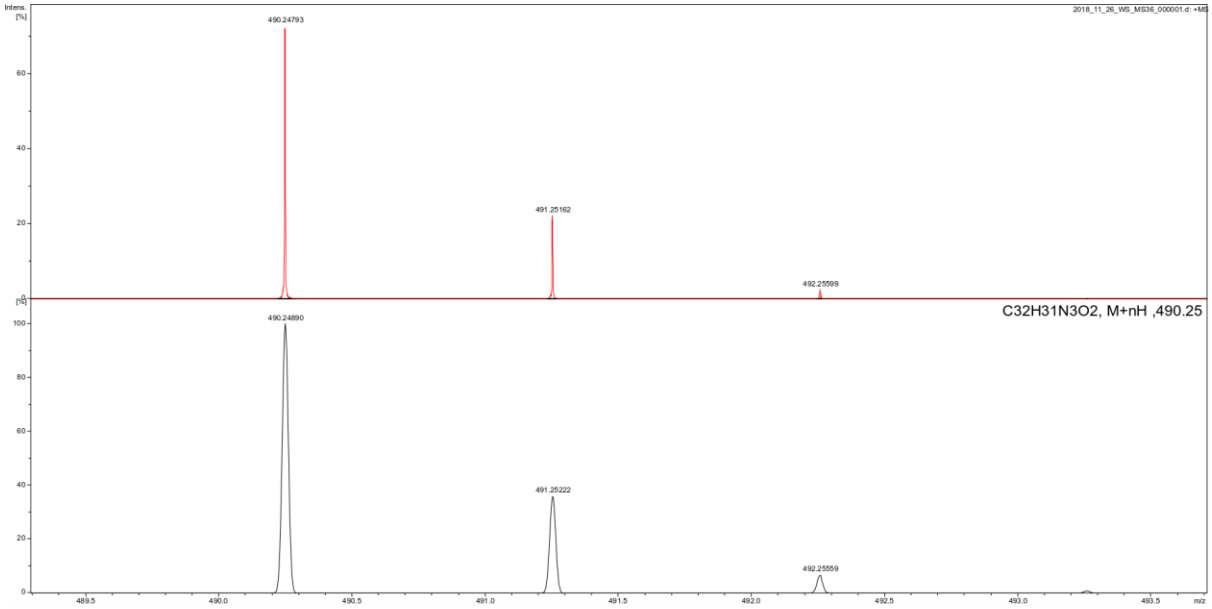

Figure S23. Mass Spectrum of **1**

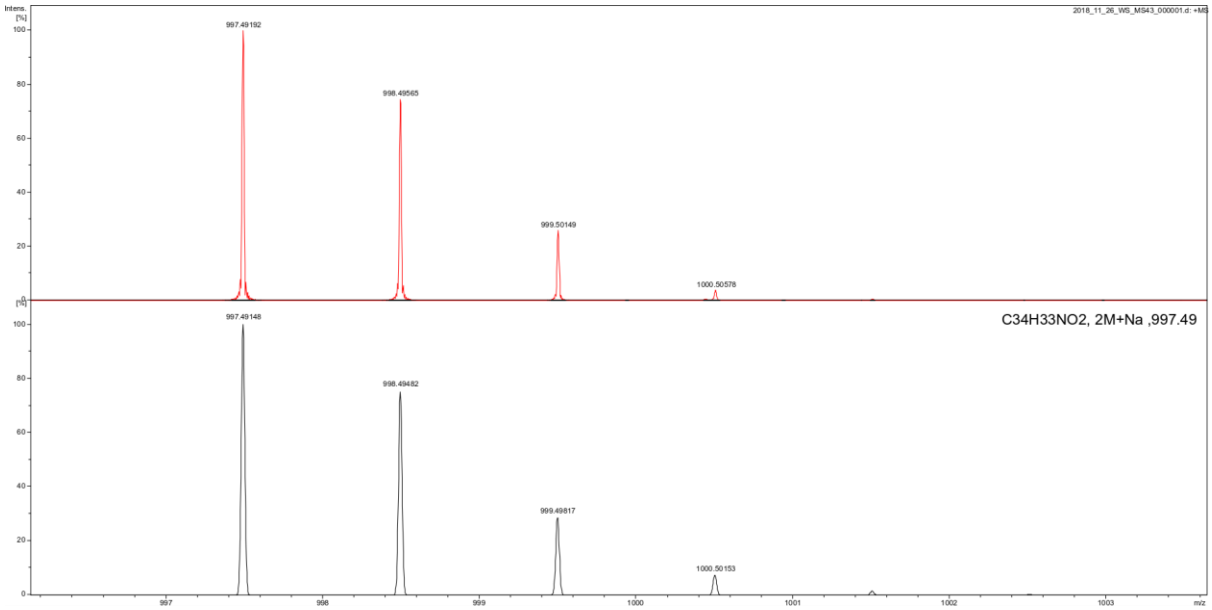

Figure S24. Mass Spectrum of **S5**

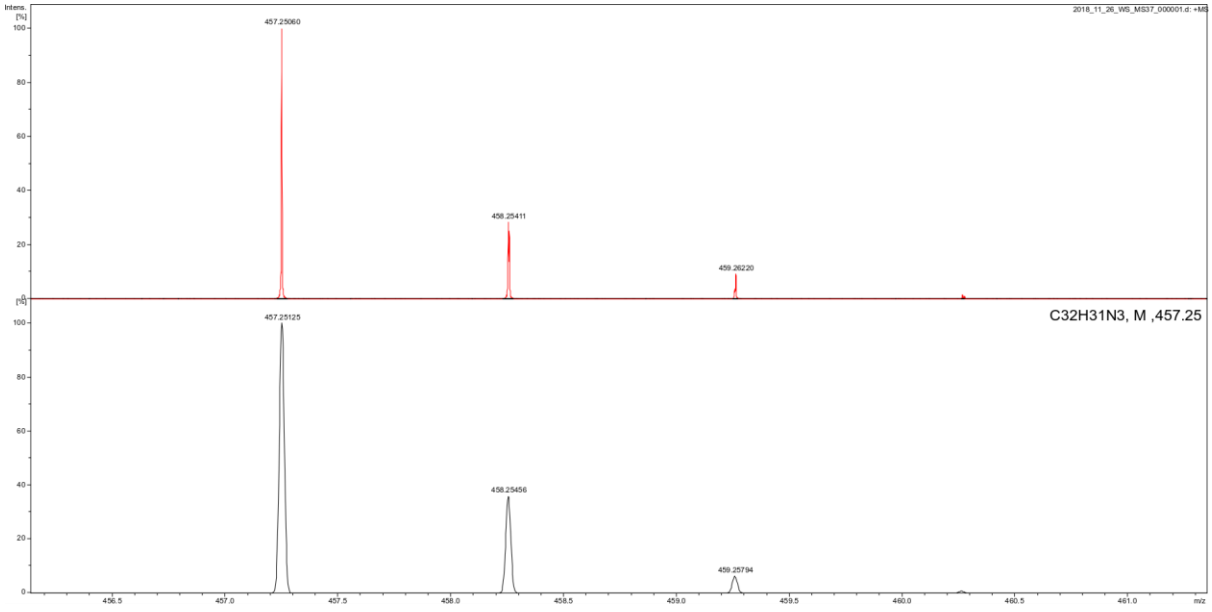

Figure S25. Mass Spectrum of **3**

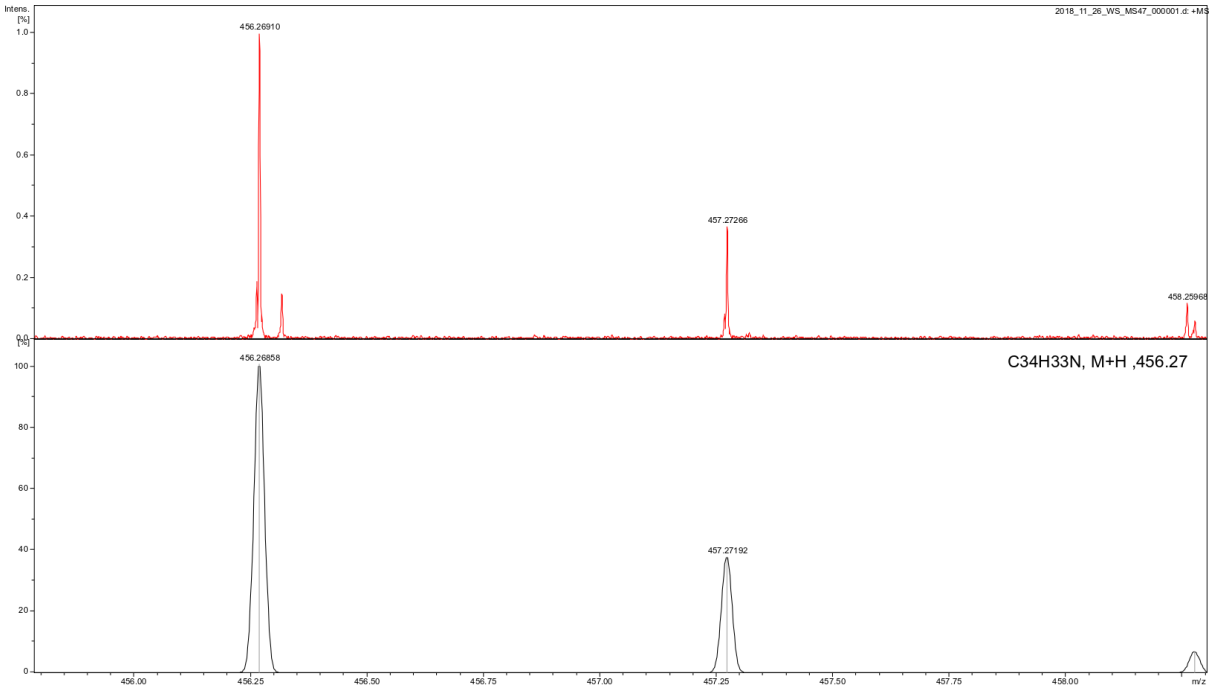

Figure S26. Mass Spectrum of **S6**

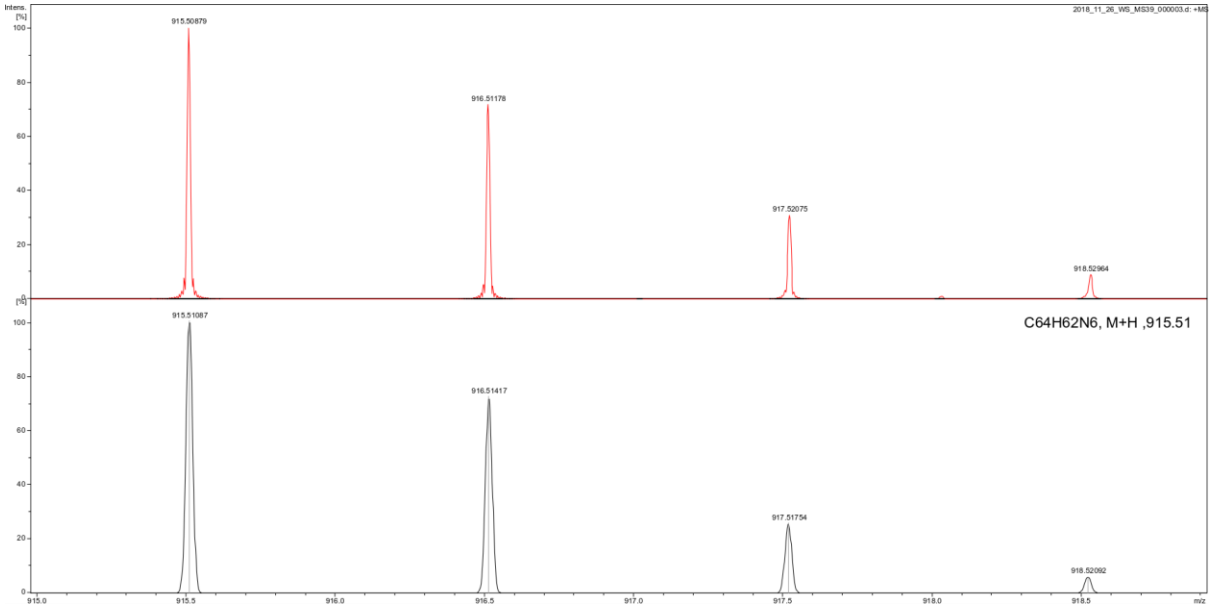

Figure S27. Mass Spectrum of **2**

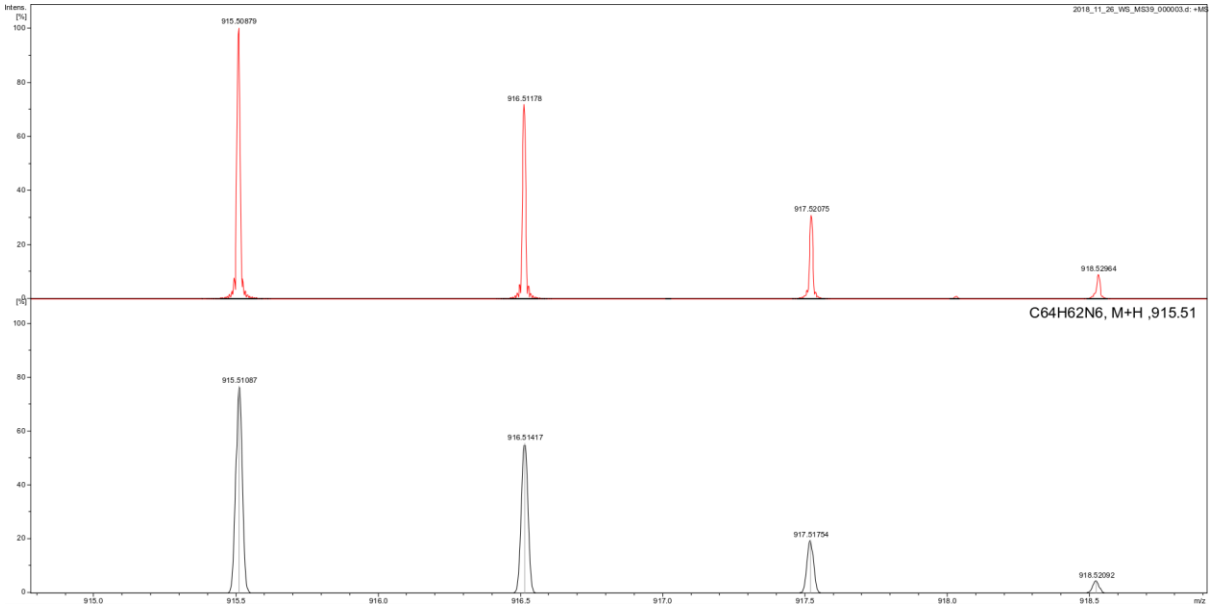

Figure S28. Mass Spectrum of **4**

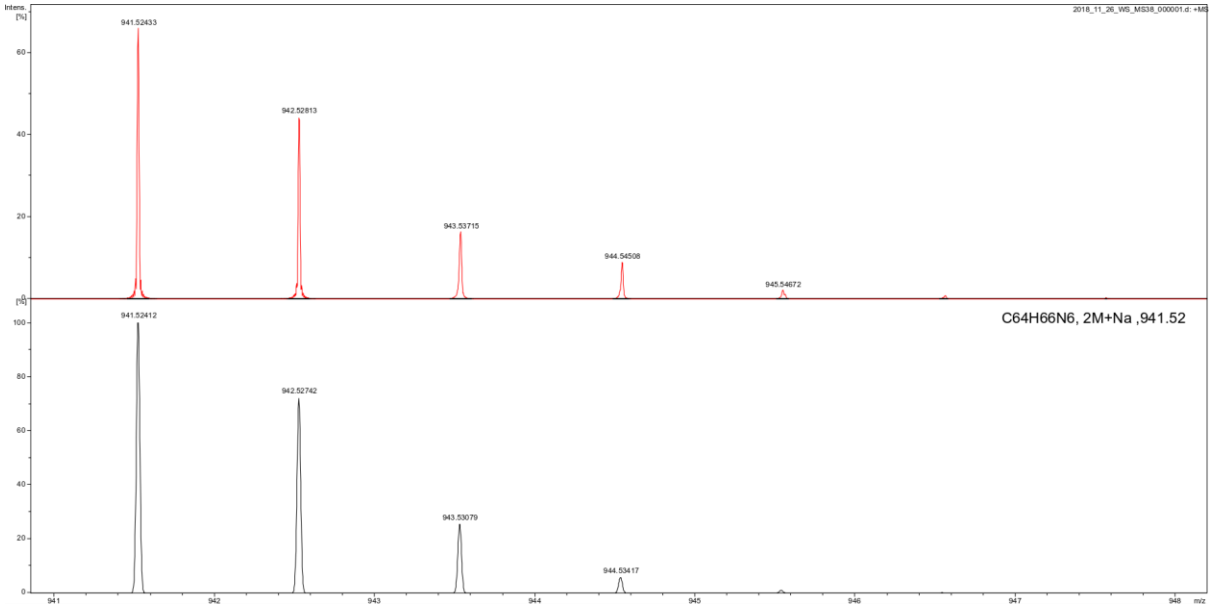

Figure S29. Mass Spectrum of **3-H_2**

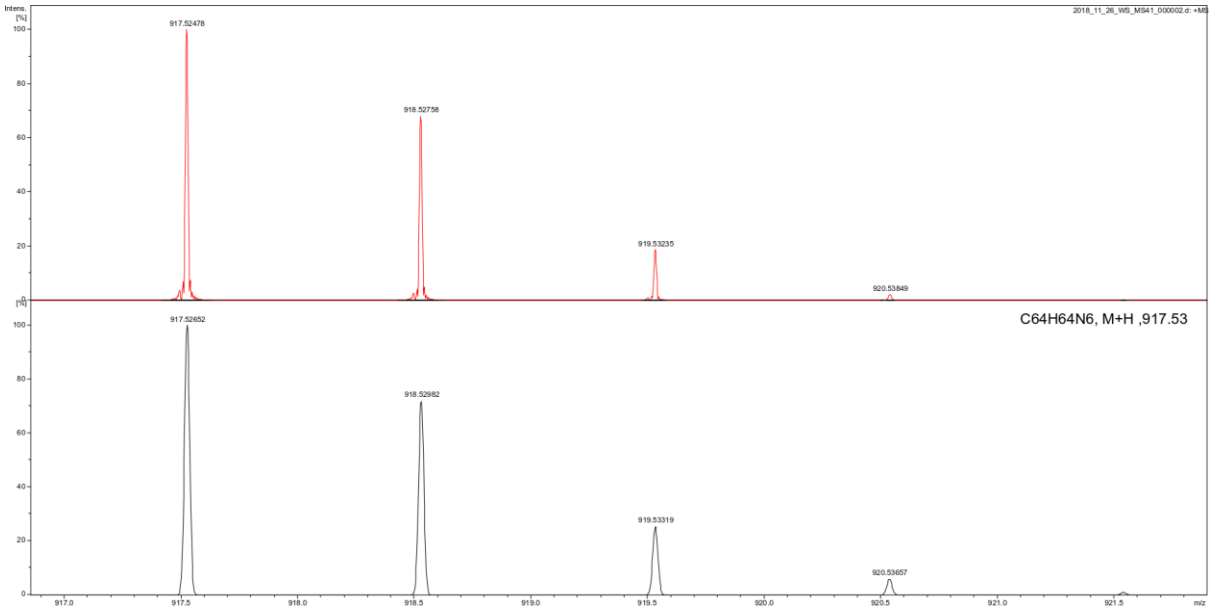

Figure S30. Mass Spectrum of **2-H_2**

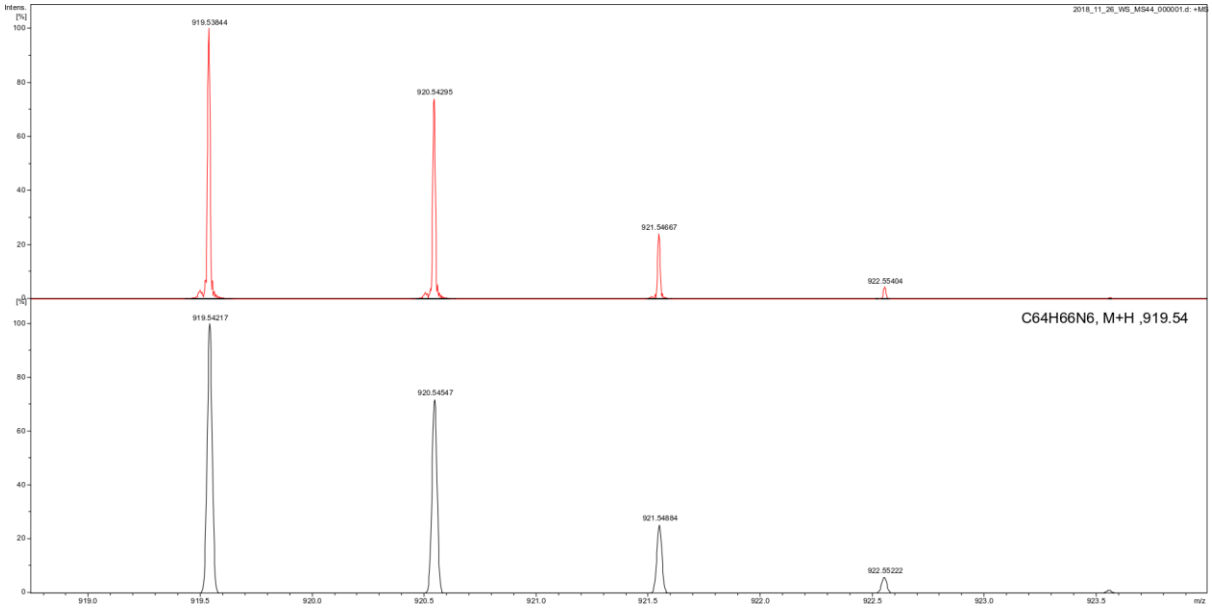

Figure S31. Mass Spectrum of **2-H$_4$**

5. X-Ray structures

Identification code	2	2-H_2	2-H_4	3	3-H_2	4
CCDC	1886974	1886970	1886973	1886967	1886969	1886972
Empirical formula	$C_{64}H_{62}N_6$	$C_{64}H_{64}N_6$	C64H66N6	$C_{32}H_{31}N_3$	$C_{66}H_{70}Cl_4N_6$	$C_{64.5}H_{62.77}Cl_{1.5}N_6$
Formula weight	915.19	917.21	917.47	457.60	1089.08	975.15
Temperature/K	100(2)	100(2)	100(2)	100(2)	100(2)	100(2)
Crystal system	monoclinic	monoclinic	monoclinic	Monoclinic	monoclinic	triclinic
Space group	C2/c	C2/c	C2/c	P21/c	$P2_1/c$	P-1
a/Å	38.154(5)	38.1618(13)	37.989(6)	16.079(2)	10.9413(2)	13.4459(9)
b/Å	10.5842(13)	10.6010(4)	10.6638(15)	13.5974(16)	16.5587(3)	22.2811(11)
c/Å	12.7576(12)	12.8755(5)	12.835(2)	11.5541(10)	31.2883(8)	23.3879(9)
α/°		90	90		90	78.605(4)
β/°	96.318(9	96.379(3)	96.415(16)	90.546(11)	98.645(2)	88.459(4)
γ/°		90	90		90	72.655(5)
Volume/$Å^3$	5120.6(10)	5176.6(3)	5167.2(14)	2526.0(5)	5604.2(2)	6552.5(6)
Z	4	4	4	4	4	4
$\rho_{calc}g/cm^3$	1.187	1.177	1.179	1.203	1.291	0.988
μ/mm^{-1}	0.534	0.069	0.069	0.541	0.259	0.117
F(000)	1952.0	1960.0	1964.0	976.0	2304.0	2069.0
Radiation	CuKα (λ = 1.54184)	MoKα (λ = 0.71073)	MoKα (λ = 0.71073)	CuKα (λ = 1.54184)	MoKα (λ = 0.71073)	MoKα (λ = 0.71073)
2Θ range for data collection/°	4.66 to 144.986	5.746 to 54.988	5.742 to 49.998	5.496 to 129.99	5.602 to 54.972	5.726 to 50
Index ranges	-47 ≤ h ≤ 42, -12 ≤ k ≤ 13, -15 ≤ l ≤ 15	-49 ≤ h ≤ 49, -13 ≤ k ≤ 13, -12 ≤ l ≤ 16	-30 ≤ h ≤ 45, -12 ≤ k ≤ 12, -15 ≤ l ≤ 15	-18 ≤ h ≤ 18, -10 ≤ k ≤ 15, -13 ≤ l ≤ 11	-14 ≤ h ≤ 13, -21 ≤ k ≤ 21, -39 ≤ l ≤ 35	-15 ≤ h ≤ 15, -26 ≤ k ≤ 26, -25 ≤ l ≤ 27
Reflections collected	13617	18859	9794	5905	35275	45474
Independent reflections	5066 [R_{int} = 0.1035, R_{sigma} = 0.1143]	5727 [R_{int} = 0.0620, R_{sigma} = 0.0589]	4510 [R_{int} = 0.1825, R_{sigma} = 0.4005]	3719 [R_{int} = 0.0610, R_{sigma} = 0.1066]	11939 [R_{int} = 0.0519, R_{sigma} = 0.0555]	22939 [R_{int} = 0.0756, R_{sigma} = 0.1798]
Data Restraints Parameters	5066/0/356	5727 0 365	4510 6 345	3719/0/322	11939 1 707	22939/1/1380
Goodness-of-fit on F^2	0.987	1.042	0.852	0.961	1.015	0.907
Final R indexes [I>=2σ (I)]	R_1 = 0.0924, wR_2 = 0.2353	R_1 = 0.0982, wR_2 = 0.2786	R_1 = 0.1041, wR_2 = 0.1864	R_1 = 0.0933, wR_2 = 0.2415	R_1 = 0.0691, wR_2 = 0.1790	R_1 = 0.1009, wR_2 = 0.2386
Final R indexes [all data]	R_1 = 0.1441, wR_2 = 0.2794	R_1 = 0.1230, wR_2 = 0.2924	R_1 = 0.3007, wR_2 = 0.2561	R_1 = 0.1422, wR_2 = 0.2844	R_1 = 0.1033, wR_2 = 0.2091	R_1 = 0.2165, wR_2 = 0.2877
Largest diff. peak/hole / e $Å^{-3}$	0.42/-0.30	0.52/-0.54	0.47/-0.31	0.27/-0.30	0.86/-0.74	0.35/-0.35

5.1. X-Ray structure of 1 and S5

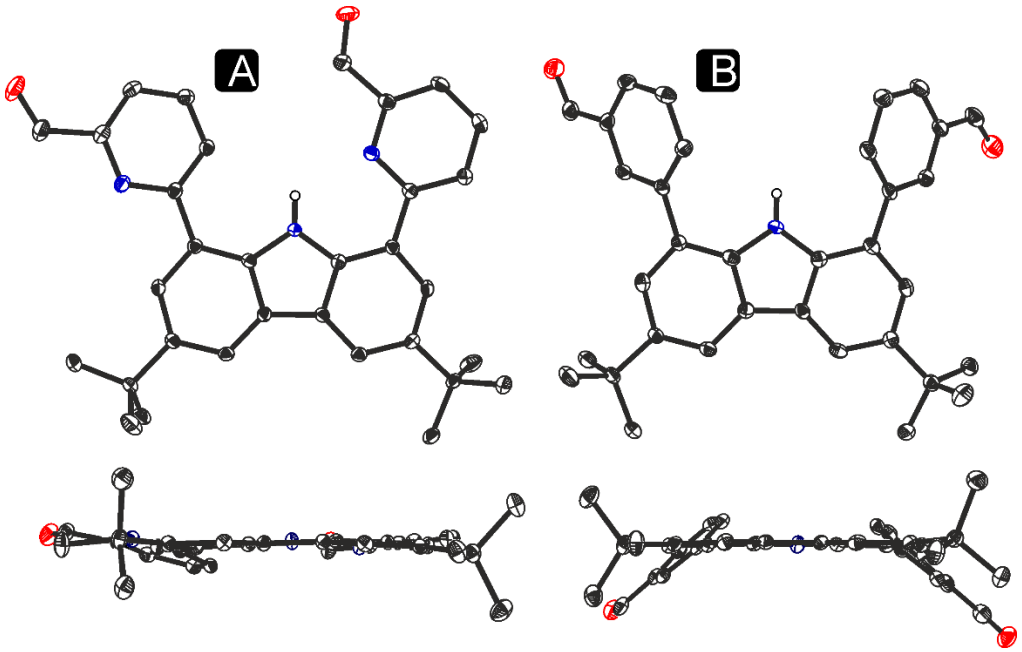

Figure S32. X-Ray structures of **1** (A) and **S5** (B)**.**

Experimental

Crystal structure determination of 1

Crystal Data for $C_{32}H_{31}N_3O_2$ (M =489.60 g/mol): triclinic, space group P-1 (no. 2), a = 9.4790(4) Å, b = 11.2211(4) Å, c = 12.2882(5) Å, α = 83.194(3)°, β = 81.408(3)°, γ = 88.438(3)°, V = 1283.19(9) Å^3, Z = 2, T = 94.97(12) K, μ(MoKα) = 0.080 mm^{-1},*Dcalc* = 1.267 g/cm^3, 19517 reflections measured (5.652° ≤ 2Θ ≤ 58.72°), 6223 unique (R_{int} = 0.0285, R_{sigma} = 0.0359) which were used in all calculations. The final R_1 was 0.0475 (I > 2σ(I)) and wR_2 was 0.1191 (all data). **CCDC 1886968**

Crystal structure determination of S5

Crystal Data for $C_{34}H_{33}NO_2$ (M =487.61 g/mol): monoclinic, space group $P2_1/c$ (no. 14), a = 18.4682(13) Å, b = 5.7331(2) Å, c = 26.1392(18) Å, β = 108.033(8)°, V = 2631.7(3) Å^3, Z = 4, T = 105(30) K, μ(MoKα) = 0.075 mm^{-1}, *Dcalc* = 1.231 g/cm^3, 11588 reflections measured (6.242° ≤ 2Θ ≤ 57.59°), 5987 unique (R_{int} = 0.0557, R_{sigma} = 0.1225) which were used in all calculations. The final R_1 was 0.0707 (I > 2σ(I)) and wR_2 was 0.1378 (all data). **CCDC 1886971**

6. CD experiments for **2**.

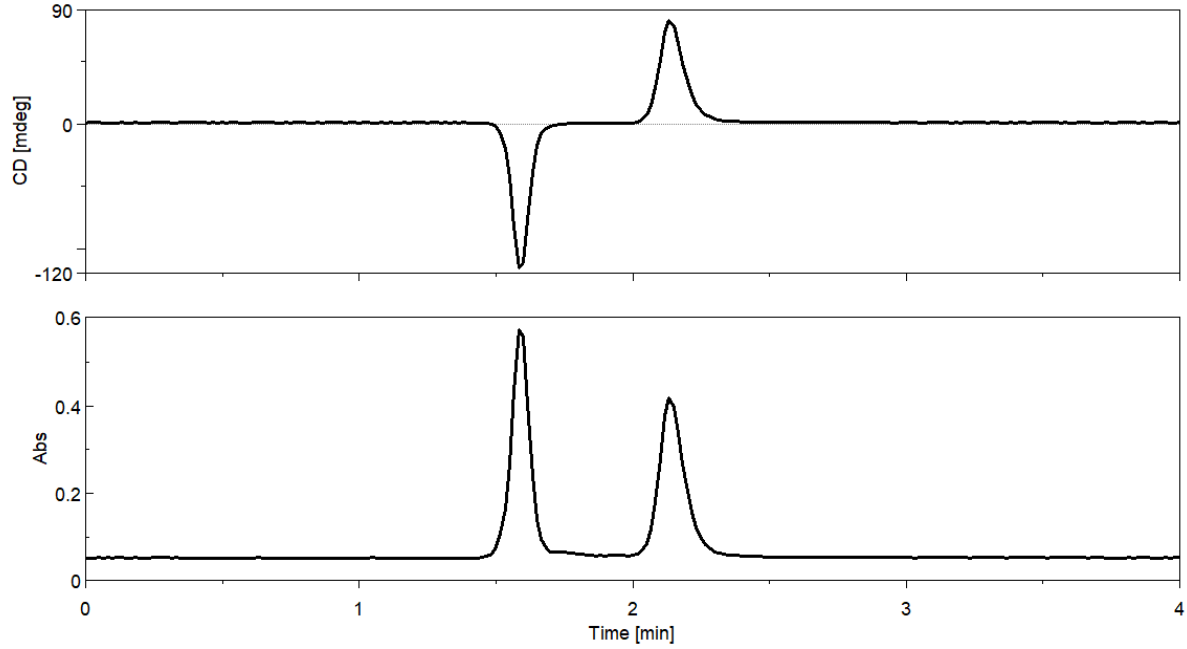

Figure S35. HPLC profiles for **2** recorded with optical absorption (lower trace) and CD (upper trace) detectors. Conditions: stationary phase, Chirex® 3010 column (250x4.6 mm); mobile phase, DCM/hexane 80/20 (v/v); flow rate, 2 ml/min; monitored wavelength, 345 nm.

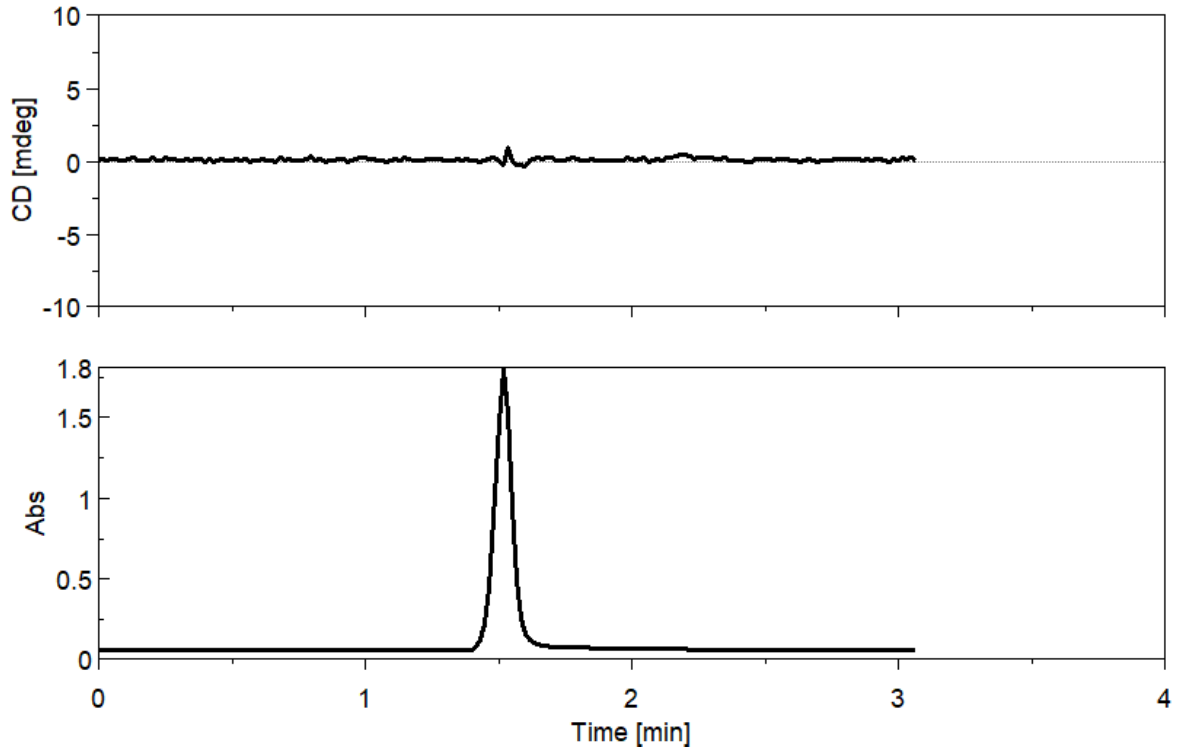

Figure S35a. HPLC profiles for **4** recorded with optical absorption (lower trace) and CD (upper trace) detectors. Conditions: stationary phase, Chirex® 3010 column (250x4.6 mm); mobile phase, DCM/hexane 80/20 (v/v); flow rate, 2 ml/min; monitored wavelength, 345 nm.

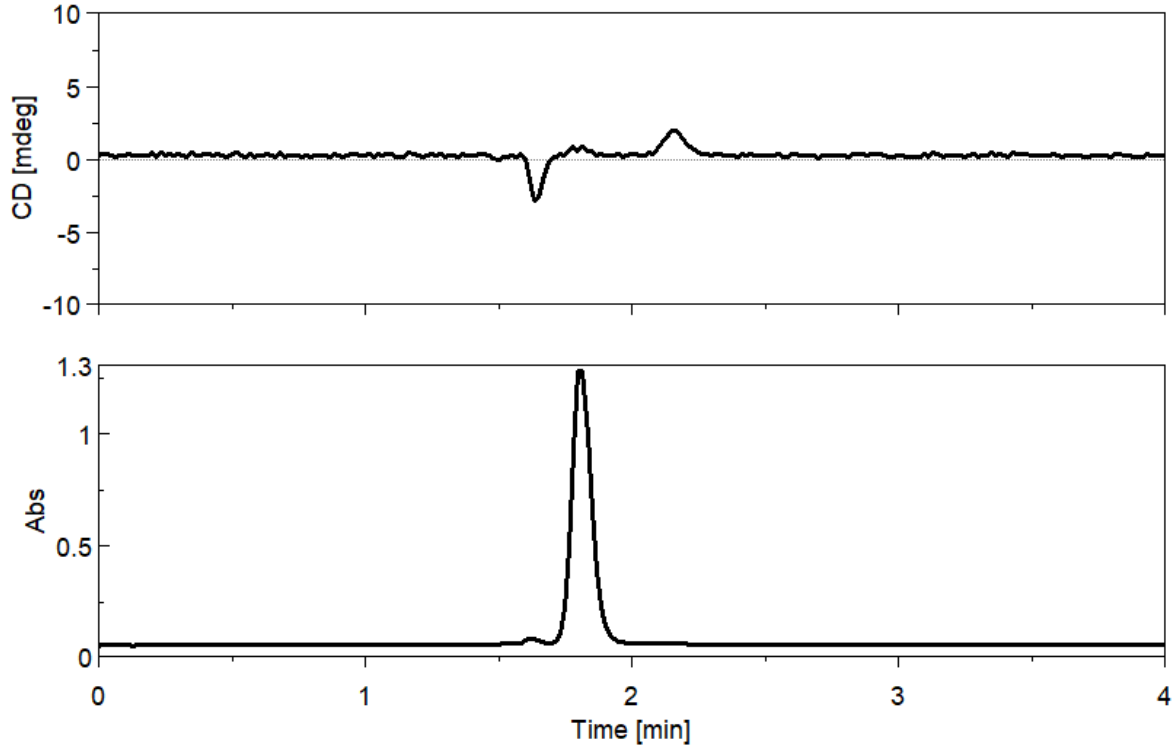

Figure S35b. HPLC profiles for **2**-H_2 recorded with optical absorption (lower trace) and CD (upper trace) detectors. Conditions: stationary phase, Chirex® 3010 column (250x4.6 mm); mobile phase, DCM/hexane 80/20 (v/v); flow rate, 2 ml/min; monitored wavelength, 345 nm. The weak peaks in the CD profile are due to a contamination of the sample with **2**.

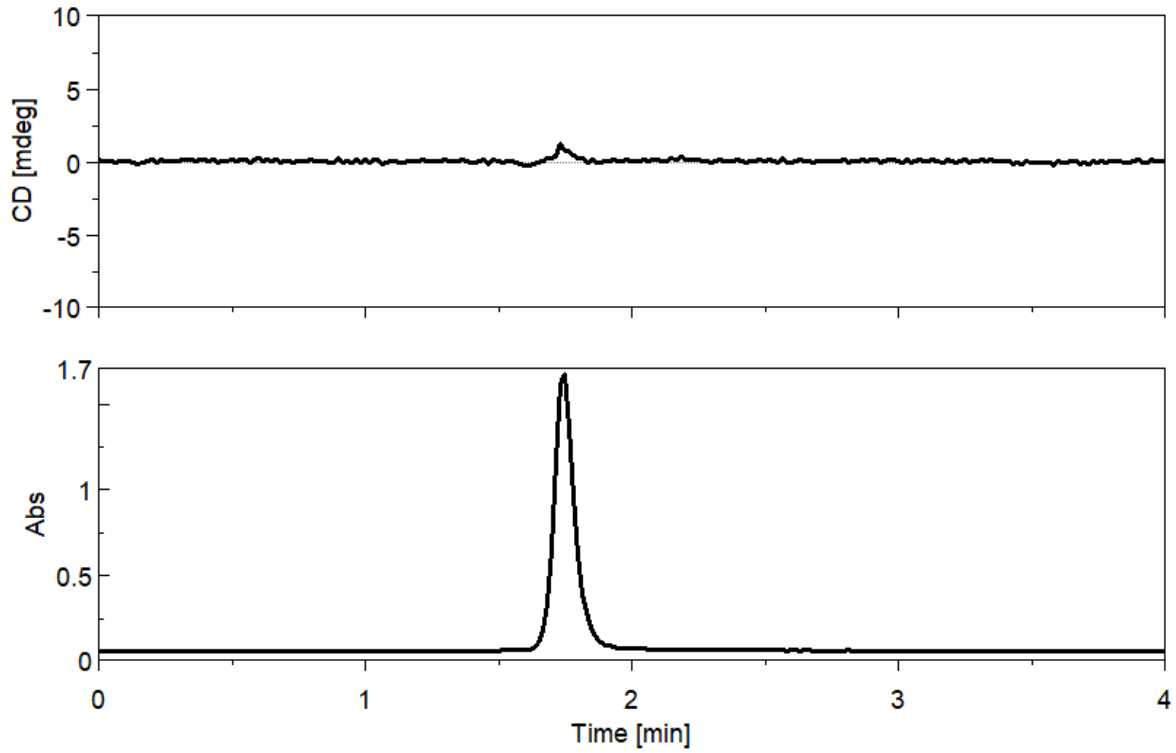

Figure S35c. HPLC profiles for **2**-H_4 recorded with optical absorption (lower trace) and CD (upper trace) detectors. Conditions: stationary phase, Chirex® 3010 column (250x4.6 mm); mobile phase, DCM/hexane 80/20 (v/v); flow rate, 2 ml/min; monitored wavelength, 345 nm.

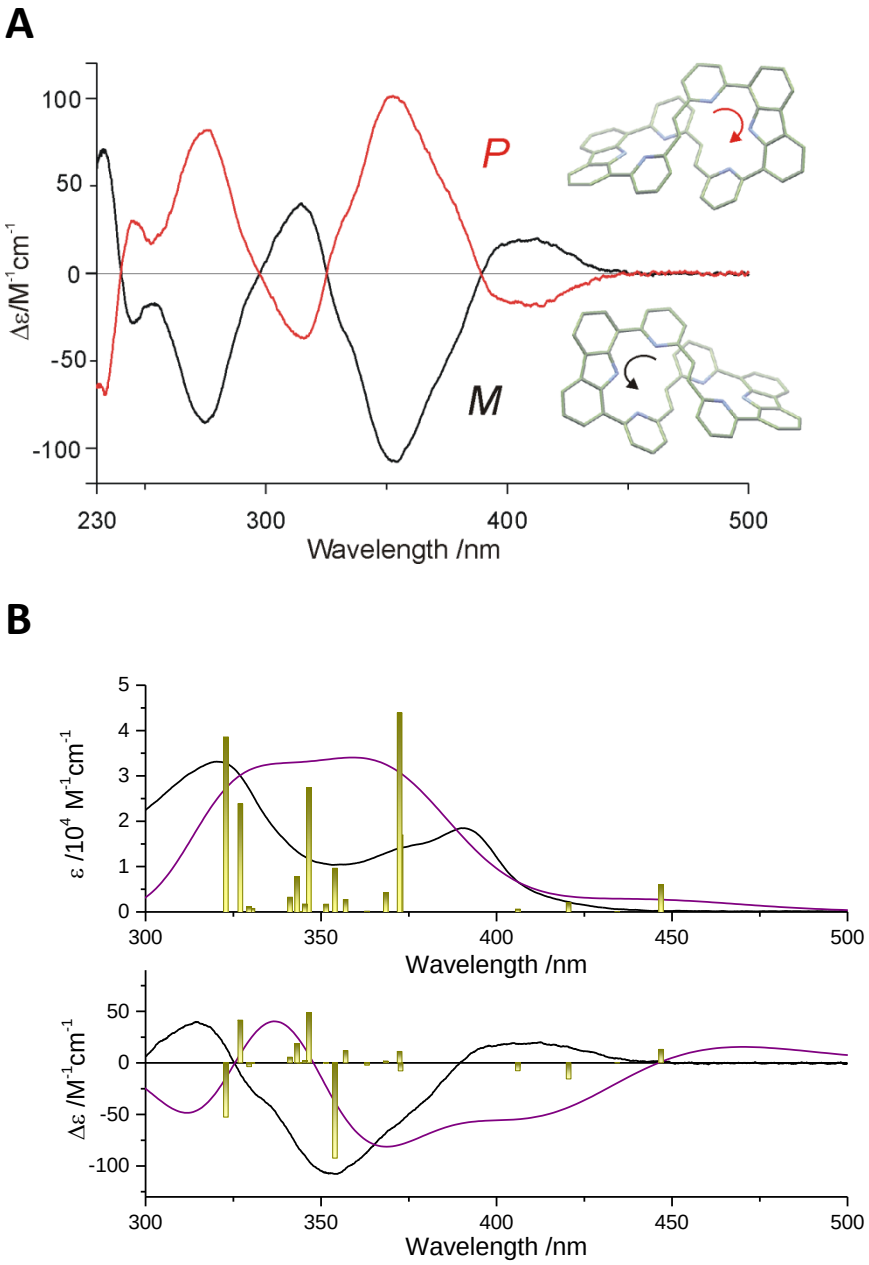

Figure S36. (A) CD spectra (298 K, DCM) of separated enantiomers of **2** along with stick representations of their skeletons and assignments of helicity senses. (B) Experimental (black) and simulated (purple) absorption (top) and CD (bottom) spectra calculated by TDDFT for a geometry-optimized structure of *M*-**2**. The shaded yellow sticks represent wavelengths of the electronic transitions and relative values of oscillator (for absorption spectra) or rotational (for CD) strengths of the transitions.

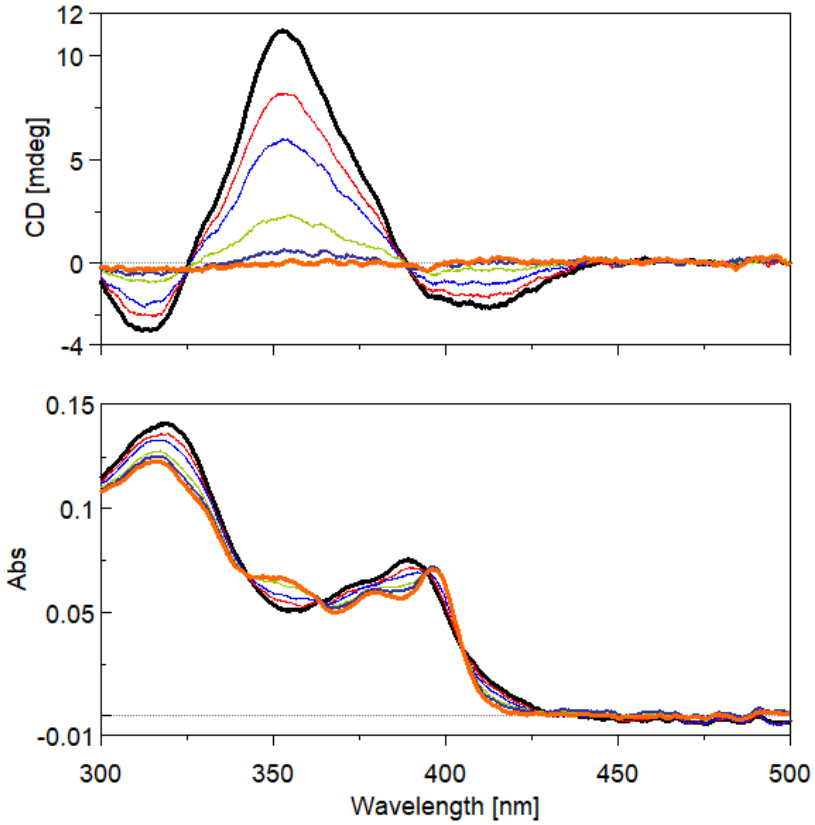

Figure S37. Time evolution of CD spectra (298 K, DCM) *P*-**2** during irradiation of the sample with 365 nm (0 min. black, 10 min. red, 20 min. blue, 50 min. green, 75 min. navy, 100 min. orange). The bottom trace presents changes of UV spectra during the experiment with a gradual appearance of **4** (orange).

7. DFT Calculations.

7.1. Optimized geometry of 2.

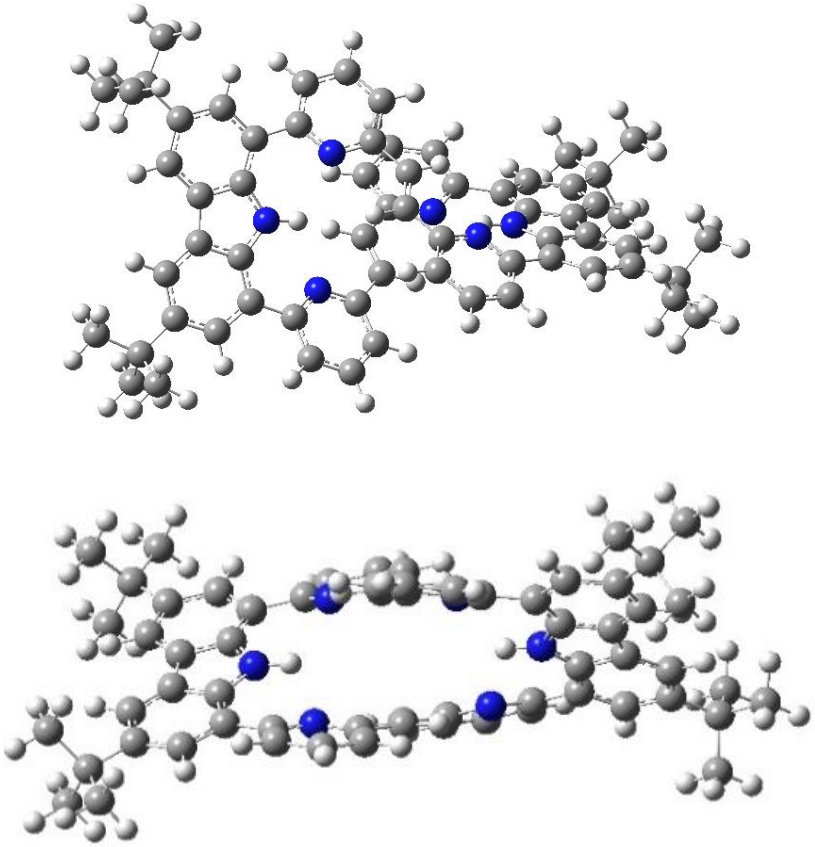

Figure S38. DFT optimized geometry of **2**.

7.2. Optimisation details

Table S1. Computational details for structures discussed in the paper. Optimizations were performed at the PCM($CHCl_3$)/B3LYP/6-31G(d,p) level of theory.

Structure	Code[a]	SCF *E*[b]	ZPV[c]	lowest freq.[d]	*G*[e]
		a.u.	a.u.	cm^{-1}	a.u.
3	JK_4a	-1402.42735447	0.552254	12.27	-1401.875101
S6	JK_4b	-1368.87634918	0.548244	29.61	-1368.328106
2	JK_5	-2804.90384917	1.105540	12.21	-2803.798310
4	JK_6	-2804.91542859	1.110889	1.43	-2803.804539
3-H_2	JK_S3	-1403.66015853	0.575601	22.87	-1403.084557
2-H_2	JK_S4	-2806.12338064	1.128580	9.20	-2804.994801
2-H_4	JK_S5	-2807.34263040	1.152146	11.27	-2806.190485

[a] Optimized geometry available as <code>.pdb file. [b] Electronic energy. [c] Zero-point vibrational energy. [d] Lowest vibrational frequency. [e] Gibbs free energy.

7.3. Calculated chemical shifts for 3, 2, 4, 3-H_2, 2-H_2, 2-H_4.

Table S2. The GIAO chemical shifts obtained for optimized structures compared with experimental values.

	3		**2**		**4**		**3-H_2**		**2-H_2**		**2-H_4**	
	Theor.	Exp.	Theor.	Exp.	Theor.	Exp.	Theor.	Exp.	Theor.	Exp.	Theor.	
Bridge	6.42	6.54	7.86 7.84 7.85 7.85	7.65	4.83 4.84 4.85 4.86	4.98	3.24 3.23	3.35	7.99 7.94 3.96 3.94 3.02 2.98	7.68 3.73 3.10	3.08 3.08 3.08 3.07 4.03 4.03 4.02 4.02	3.41
4,17	7.16	7.19	6.70 6.69 6.69 6.69	6.41	6.94 6.94 6.95 6.94	6.80	7.24	7.12	6.82 6.79 6.76 6.76	6.51 6.48	6.88 6.86 6.86 6.86	6.54
5,16	7.82	7.75	7.71 7.69 7.68 7.68	7.52	7.68 7.68 7.68 7.68	7.55	7.88	7.75	7.71 7.69 7.65 7.63	7.55 7.49	7.67 7.65 7.65 7.64	7.47
6,15	8.04	7.93	7.84 7.82 7.82 7.82	7.80	8.25 8.25 8.25 8.25	8.03	8.10	7.91	7.87 7.87 7.87 7.83	7.80 7.76	7.93 7.90 7.90 7.89	7.77
8^1,13^1	8.41	8.18	8.28 8.02 8.02 8.01	7.95	8.68 8.68 8.68 8.68	8.32	8.46	8.22	8.28 8.05 8.02 7.99	7.93 7.91	8.31 8.05 8.04 8.04	7.90
10^1,11^1	8.22	7.97	8.71 8.71 8.68 8.41	8.27	8.42 8.42 8.42 8.42	8.23	8.29	8.03	8.71 8.69 8.66 8.41	8.26 8.24	8.40 8.67 8.70 8.70	8.25
NH	17.37	17.78	12.08 12.05	12.84	14.20 14.20	14.67	15.91	16.32	11.84 11.83	12.32	11.62 11.64	11.88

8. UV-Vis and Fluorescence spectra.

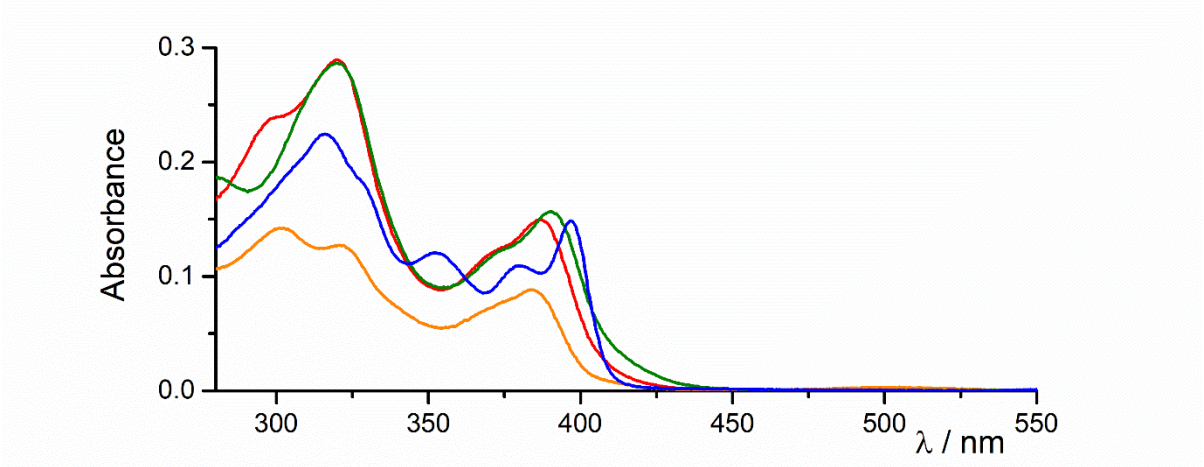

Figure S39. Absorption spectra of **2** (green), **2-H$_2$** (red), **2-H$_4$** (orange) and **4** (blue) (CH_2Cl_2, 298 K).

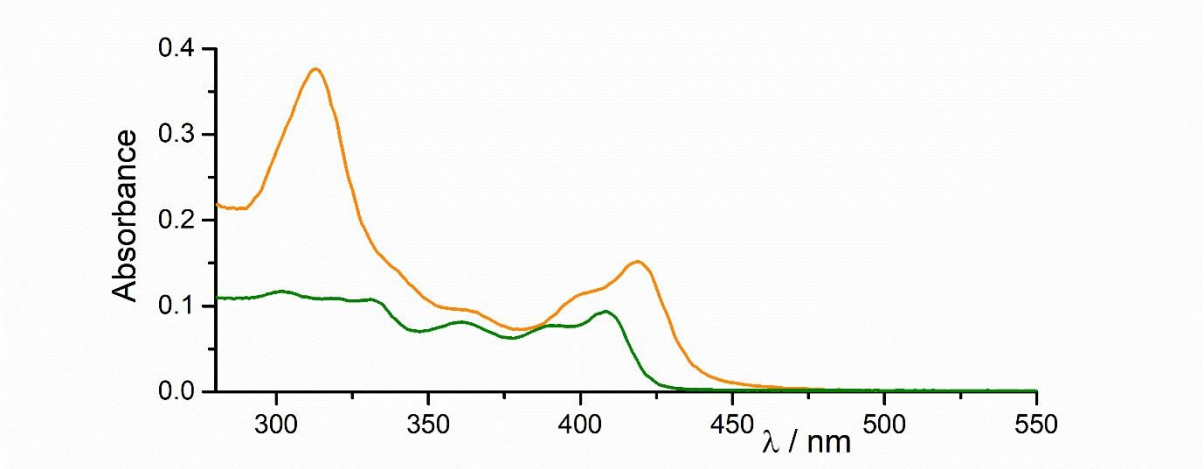

Figure S40. Absorption spectra of **3** (orange) and **3-H$_2$** (green) (CH_2Cl_2, 298 K).

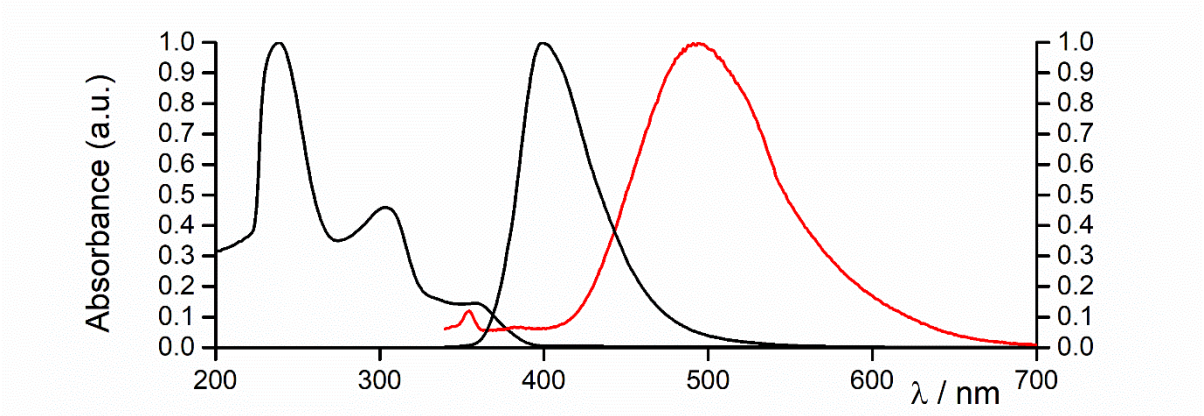

Figure S41. Absorption and emission spectra of **S6** (black) and **S5** (red) (CH_2Cl_2, 298 K).

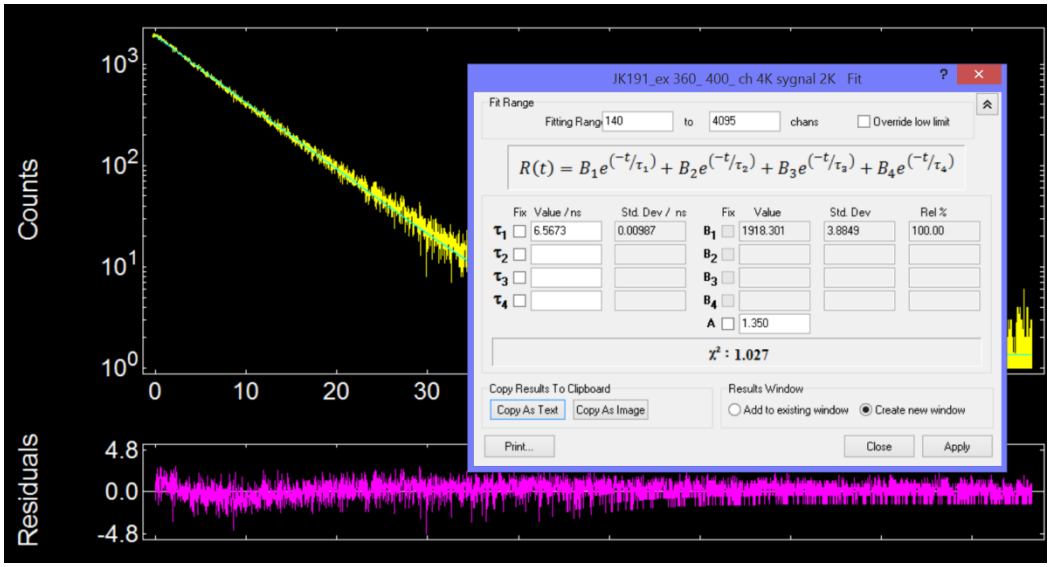

Figure S42. Decay profile of **S6** (black) (CH_2Cl_2, 298 K, Excitation 360 nm detection 400 nm).

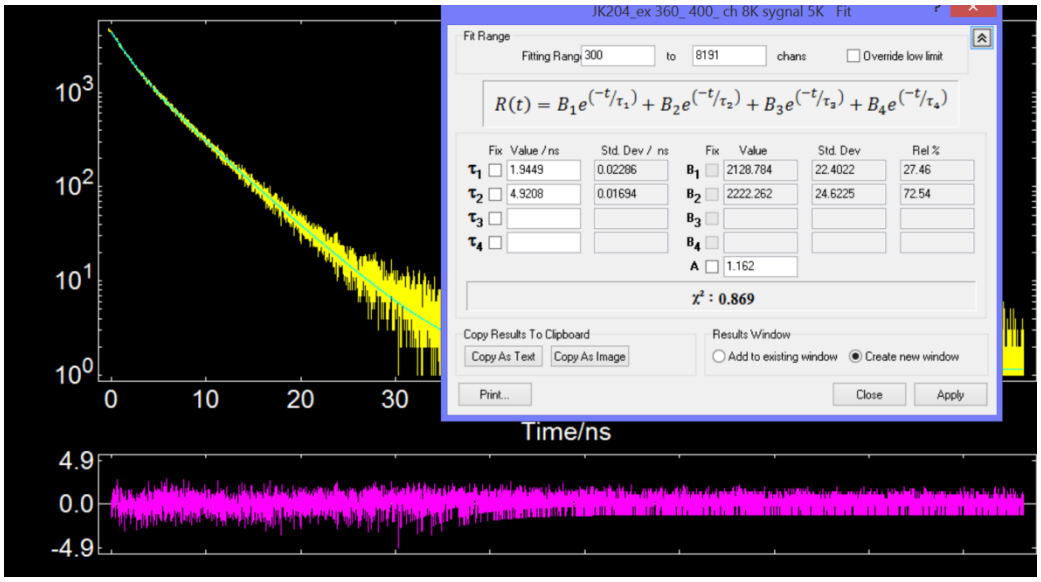

Figure S43. Decay profile of **S5** (black) (CH_2Cl_2, 298 K, Excitation 360 nm detection 490 nm).